Norwegian University of Life Sciences
Faculty of Environmental Science and Technology
Department of Mathematical Sciences and Technology

Master Thesis 2015
30 credits

Removal of Phosphate from Wastewater by Adsorption onto Composite made from Chitosan and Calcium Carbonate

Morten Sørby

This thesis is part of a cross-disciplinary project at NMBU, where the goal is to explore different methods for removing low concentrations of phosphate from effluent water.

This thesis will look at how a mix of sea shells and other calcium rich husks from mollusks can be used as a component in a biologically degradable adsorbent for removing phosphates.

The process of putting this thesis together has been an opportunity to learn new things and I have experienced how this education is just a starting point for future work experience, where the education never really end. A big part of the motivation has been to have the opportunity to explore ways of solving a practical problem and find out how to put this patchwork of an education to use.

I have been given a good portion of freedom to shape this thesis myself, for which I am very grateful to my patient supervisors John Erlend Mosbye, Olav Kraugerud and Odd Ivar Lekang.

I would also like to thank Harald Støkken, Bjørn Reidar Hansen and Bjørn Frode Eriksen which have helped my out underway.

I am also grateful to my friends and family who have supported me through this education.

13.05.2015 Morten Sørby

Forord

Oppgaven er en masteroppgave i prosessteknikk ved NMBU og er del av et tverrfaglig prosjekt ved NMBU hvor målet er å utforske metoder for å fange lave konsentrasjoner av fosfor fra avløpsvann.

Oppgaven tar for seg bruk av skjellsand og chitosan som blir brukt til å lage et materiale som kan fungere som en biologisk nedbrytbar adsorbent for fosfater.

Arbeidet med denne oppgaven har vært en veldig lærerik periode hvor jeg har fått erfare at dette virkelig er en type utdannelse som kun fungerer som en startpakke for veien videre, hvor man aldri blir ferdig utlært. En stor del av motivasjonen har vært å kunne sette seg inn i en praktisk problemstilling, lære mye nytt og se hvordan det egentlig fungerer når man skal bruke en utdannelse som stort sett er et lappeteppe av varierte kunnskaper.

Jeg har fått stor frihet til å forme oppgaven selv og skylder en stor takk til mine tålmodige veiledere John Erlend Mosbye, Olav Kraugerud og Odd Ivar Lekang.

Jeg vil også takke Harald Støkken, Bjørn Reidar Hansen og Bjørn Frode Eriksen som har bidratt med innføring, støtte og innspill på fiskelabben.

Jeg skylder også en stor takk til familie og venner som har støttet meg underveis.

13.05.2015 Morten Sørby

Abstract

Calcium carbonate in the form of calcite and aragonite has previously shown potential for removing low concentrations of phosphate from wastewater. This project look at how calcium carbonate can be used to make an adsorbent that belong to a fairly new class of composite adsorbents that utilizes chitosan and inorganic materials. The motivation for using a composite instead of calcium carbonate alone is that this minerals ability to adsorb phosphate is surface specific. In order to maximize the amount of available surface area, the calcite and aragonite will need to be milled extensively into a very fine powder which makes in impractical to separate from water in larger scale.

Table of Contents

1.0 Introduction

The main issue with phosphorus today is that we have become dependent on spending far more than we are able to recycle, as a result of this we are depleting the deposits of phosphate rich minerals found around the world.

When it comes to recycling phosphorus the portion of it that is bound in organic matter is the easiest to capture and recycle, this can be done by separating sediments from waste water and utilizing biological filter systems. Unfortunately there is often a portion of the phosphorus that still escapes with the waste water, this phosphorus is commonly in the form of low concentrations of phosphates.

There exist several viable options for removing this phosphate today but, the challenge is to find methods that are less expensive in terms of equipment, energy demand and maintenance.

One low cost resource that has been found to adsorb low concentrations of phosphate in water is the mineral form of calcium carbonate.

The topic of this thesis is to study how calcium carbonate in the form of a mixture of sea shells and husks from mollusks can be prepared to make a new composite material that can be able to adsorb low concentrations of phosphate in waste water.

Phosphate in wastewater

The fish feed used in aquaculture can contain up to 1.5 percent phosphates, the fish only use 30 percent of this amount however, the rest is excreted along with the digested feed. In the future, new facilities in aquaculture will be built on land which opens up new opportunities when it comes to recycling the remaining 70 percent of the phosphate that get lost today.

There are several types of materials that can be used at adsorbents to remove phosphate from effluent water, some can be used in a cyclic process where the material is stripped of phosphate and recycled, commonly referred to as *regenerated*. Other materials like calcium minerals, can only be used once, although afterwards they can used for agriculture as a soil additive.

Adsorbents

If the calcium carbonate, in the form of a substrate made from sea shells, is applied alone then there will be a number of challenges when it comes to separating this shell substrate from the waste water afterwards.

The mechanism behind how this shell substrate adsorb the phosphate is related to the materials surface area, the more combined surface area the individual particles have, the more phosphate is is likely to adsorb. This material property, the amount of combined surface area it contains, is commonly referred to as *specific surface area* often given in square meters per gram (m^2/g).

If the substrate has been milled down to a fine powder, then there will be a challenge when it comes to finding a way to apply this powdered material efficiently, especially with large volumes of water.

These fine particles can act as colloids, which means they will stay suspended in the water for a while before they eventually stick together (flocculate) and sink to bottom. Two common ways of solving this problem is to either use large sedimentation tanks or the water can be run through

a centrifuge. It can also be a challenge to use these solutions economically since sedimentation tanks require large volumes while centrifuges can have a high demand for energy.

Fortunately there has been done promising experiments (Auta, Hameed, 2013), where one type of adsorbent substrate has been combined with a permeable polymer to form a new composite material without sacrificing any surface specific properties. With these types of composite materials, smaller particles at the molecular scale are allowed to diffuse through the polymer with little effort, but larger particles are neither able to travel in or to escape.

When the new composite material is molded into individual units, often called *beads*, the adsorption rate may not work quite as fast if we compare them to the individual components alone. However, these units will be large enough to separate from running water in a far more practical way than any powdered material.

The advantages and drawbacks of using beads for an adsorption process is given below:

Motivation for using beads, advantages of adsorbent type process'

- Tolerance for fluctuations in feed flow
- Fast adsorptive reaction process.
- Simple process operation.
- Simple to scale for higher flow rates.
- Relatively easy to modify bead properties, bead composition can be tailored to make the most of local conditions.
- The process needs both less volume than sedimentation tanks and less energy than industrial scale centrifuges.
- Adsorption beads are fairly inexpensive to produce.
- The beads can be made biologically degradable and non-toxic to the environment.

Limitations and drawbacks with adsorbent beads

- Suspended particles can cause channel formation and clogging, the beads may get coated by organic debris and other fine suspended particles. Residual particles from bead production can both initiate flocculation and formation of channels (*channeling)*.
- The beads may also able to adsorb undesired compounds and other pollutants.
- Beads often need a short pretreatment, in many cases this involves time to swell with water before they are ready to be used efficiently, although this is often only a minor drawback.

Why chitosan?

The polymer of choice for this project is chitosan. It meets the criteria listed above and it is one of the least expensive bio-degradable polymers on the marked today.

Regarding methods

In this project the experiments are intended as screening of a new combination of two known materials. The scope was to find a few central properties out of many the many possible ones.

The first steps will also involve getting a decent overview regarding how the individual parts behave on their own, after this is done it is easier to find a reasonable starting point before making different ratios and compositions of the two components.

2.0 Theory

2.1 Analysis of particle size

Each of the sieved fractions were analyzed for distribution of particle sizes, this was done with a *Mastersizer* instrument from *Malvern Instruments,* which measure particle sizes through light diffraction.

The following section is based on Malvern Instruments documentation (1997) for the Mastersizer instrument:

The Mastersizer instrument use the principle that small particles will scatter and absorb light differently depending on their size. The shape and size of a particle will determine its pattern of light scattering which will be different to any particle that is even marginally smaller or larger. This effect give it a fairly specific signature which can be used to approximate its size. The instrument detects groups of pattern that are very similar label them as signals which are then sorted into a long list, each signal will be equivalent of a small span of particle sizes. The intensity of each signal will show which scattering patterns that dominate, this tells us which groups particle sizes that make up the most significant portions of the volume of a sample.

This instrument has to use a model where the particles shape needs to be simplified to resemble a more or less symmetric geometric shape, this can be spheres, discs, cylinders and so on. In the model most commonly used by this instrument, the particles are assumed to be shaped as discs in order to approximate their size.

The size distribution is based on equivalent volumes, in other words the tables show calculated values in terms of percentage of volume. Each span of particle size is shown in terms of the volume they occupy.

The data obtained in this type of analysis give important information of the outer surface area, unfortunately this is does not include the surface area included in any pore structures the particles may have. The pore structure of materials like mollusk shells may be significant enough to have some impact on the accuracy of this type of analysis. It is still hard to imagine it will cause any dramatic difference between surface area estimated from light scattering data and the actual amount of surface area, *(Malvern Instruments, 1997).*

Malvern Instruments, Mastersizer: Explanation of result parameters

Specific surface area, α [m²/g]

This is outer surface of the particles estimated by the software.

Obscuration

If the sample is too dense the diffracted light will not sufficiently reach the sensor, obscuration can in other words affect the accuracy of the measurements.

Surface weighted mean/Sauter mean diamter D[3, 2]

This is defined as "*the diameter of a sphere that has the same volume/surface area ratio as a particle of interest." [wikipedia]*

Volume Weighted Mean/Sauter mean diamter D[4,3]

Similar to the above, but with volume as the parameter "*the diameter of a sphere that has the same volume/surface area ratio as a particle of interest." [wikipedia]*

Uniformity

This measure the absolute deviation from the median, in other words how much variation there is in size compared to the groups of particles that are most dominating in the sample volume.

Concentration, %Volume

"This value represent the volume concentration and is calculated from Beer-Lambert law and is expressed as a percentage."

Obscuration

This is a measure of how much intensity is absorbed from the lazer beam when the sample first enters the system. This value is ideally between 10 to 30 percent. [ref]

D(v, 0.5), D(v, 0.1) and D(v, 0.9)

These are "the standard "percentile" readings from the analysis.

- *D(v, 0.5) is the size of particle at which 50% of the sample is smaller and 50% is larger than this size. This value is also known as the Mass median diameter (MMD).*
- *D(v, 0.1) is the size of particle for which 10% of the sample is below this size.*
- *D(v, 0.9) gives a size of particle for which 90% of the sample is below this size. " [ref]*

D[4,3]

"This is the volume mean diameter. "

D[3,2]

"This is the surface area mean diameter. Also known as the Sauter mean."

Span

"Span is the measurement of the width of the distribution. The smaller the value the narrower the distribution."

The width is calculated as:

$$\frac{d(0.9)-d(0.1)}{d(0.5)}$$

Distribution
"This tells you the type of distribution the analysis has used. The options for this is set in the Result modification dialogue in the Setup menu. Options include change from volume to surface area, length or number. It must be remembered that the Mastersizer measurement is fundamentally a volume distribution - transforming the result into a surface, length or number distribution is a mathematical process that may amplify any error in the original result."(Malvern Instruments, 1997).

2.2 Analysis of phosphate concentrations – Merck Spectroquant Nova60

This instrument uses photometry to detect the presence of phosphate that has reacted with indicator compounds in the sample.

The following section is based on the documentation for the instrument Merck Spectroquant Nova60 (2009) and Phosphate cell test (2011):

When a light beam is sent through a water sample, certain wavelengths of the light beam will loose more intensity than others. The same phenomena can be seen with plant leaves which adsorbs red, yellow and blue light while green is reflected back.

When the indicator compounds react with inorganic phosphate, a new product is formed that has its own signature in the way that it reduce the intensity of specific wavelengths, when the light beam pass though a sample the loss of intensity in these wavelengths will be proportional to the concentration of these new species.

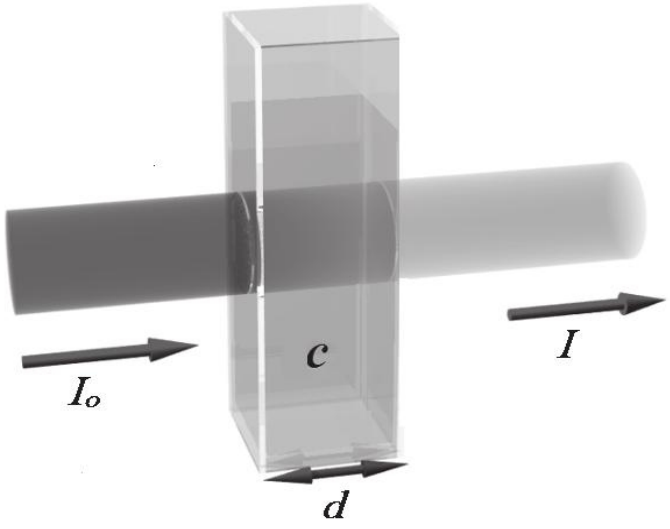

Figure. 2.1 – Light adsorption though a test sample. Courtesy of Merck instruments (2009).

The instrument has monochromatic filters that remove any wavelength that will not be absorbed by the sample, so that the light beam only contain "useful" wavelengths before it pass through the sample. In this way, only the average loss of light intensity needs to measured.

This change in intensity is expressed as:

$$T = \frac{I}{I_0}$$

T = Transmittance
I = Intensity
I_0 = Initial intensity

The total light absorption **A** is the negative logarithm of the transmittance **T**:

$$\mathbf{A = - \log T}$$

The concentration **c**, is related to the adsorption **A** through:

$$\mathbf{A = \varepsilon_\lambda * c * d}$$

$\boldsymbol{\varepsilon_\lambda}$ = molar absorptivity (l/mol*cm)
c = concentration of analyte in moles
d = length of sample cell in centimeters

Accuracy

Both physical parameters and chemical conditions can affect the accuracy of the measurements.

Temperature
The test kit will be most accurate within a temperature interval of 15^{o}C and 30^{o}C, outside this temperature span the absorbency will quickly drop.

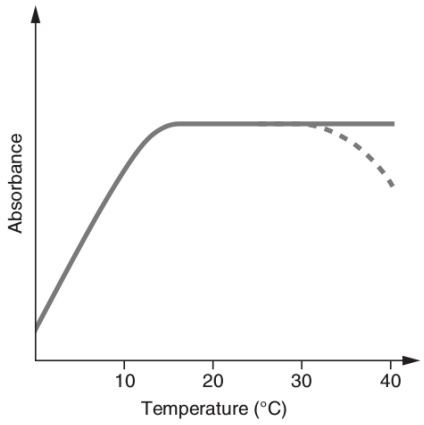

Turbidity
If the sample has a significant of suspended particles the measured value is likely to be fairly useless. This is easily taken of by running the sample water through a syringe filter before adding any reagents.

Influence of pH
According to the manufacturer the reagents are buffered so that natural fluctuation in pH are harmless.

Figure 2.2 – Courtesy of Merck instruments.

"*The reagents contained in the test kits produce an adequate buffering of the sample solutions and ensure that the pH optimal for the reaction in question is obtained*." *(Merc, 2009, Ch.1).*

2.3 Seashells as a source of aragonite and calcite

The main component in shells from marine invertebrates like blue mussels, oysters and aquatic snails is calcium carbonate. These invertebrates mainly use two crystal forms of calcium carbonate which are aragonite and calcite. The shells are made up of complex structures of either calcite or aragonite crystals which are woven into a matrix of protein fibers. The minerals are hard and brittle though excellent against compressive forces, while protein fibers give tensile strength. Aragonite and calcite give these shells their chalky white texture.[5]

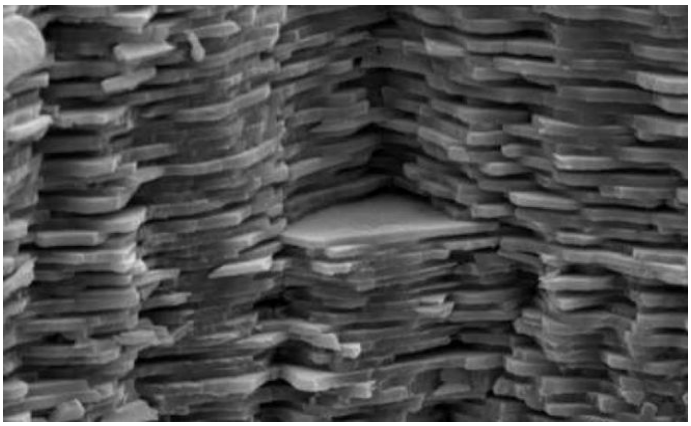

Figure. 2.3: Aragonite form layered discs in a mollusk shell. [5]

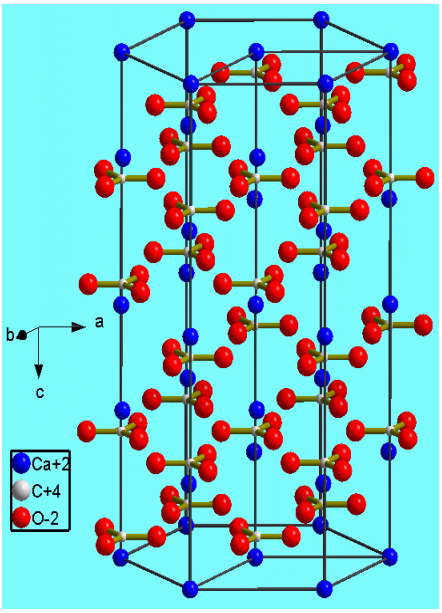

Figure 2.5: Calcite crystal structure.[5]

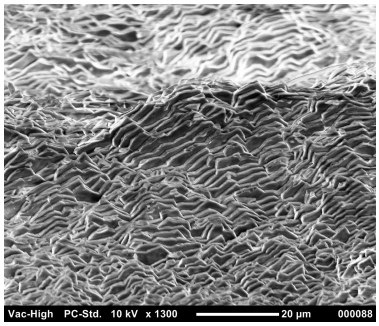

Figure 2.4: Aragonite in an oyster shell, individual mollusk species often use one of the two crystal structures.[5]

2.4 Chitosan

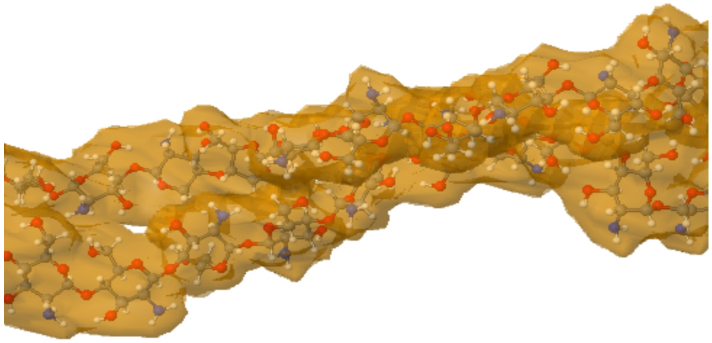

Figure. 2.7: Backplate of a crab shell, like with other crustaceans shells chitin is the chief component. [6]

Figure. 2.6: Chitosan chains shown with volumetric radius (software, 2015).

The following section is based on the articles about chitosan and chitin from wikipedia (2014):

The organic polymer chitosan is a naturally occurring byproduct of chitin, one of the most common polymers in nature where it makes up the cell walls in fungus and the exoskeleton of insects, spiders, crustaceans and other body parts in invertebrates.[6]

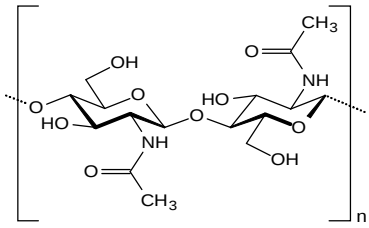

Figure. 2.8: General structure of chitin[7] *Fig. 2.9-2.11: Crustaceans shells from the seafood industry provides raw chitin[7]*

The waste from the seafood industry are one of the main sources of raw material for chitosan production.

Chitin is a polymer made of polymerized N-acetylglucosamine, forming straight linear chains. The acetyl group on each amine increase hydrogen bonds between the chains, giving the polymer more tensile strength.[7]

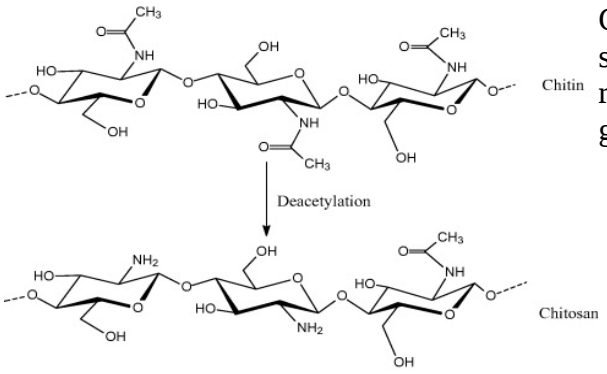

Chitosan is made by treating chitin with heat and sodium hydroxide. This initiate a deacetylation reaction, which like name implies, strip the amine groups of their acetyl groups.[6]

Figure 2.12: Structural changes after chitin is converted to chitosan[6]

Chitosans properties

Chitosan is hydrophilic at neutral to slightly alkaline conditions, at slightly acidic conditions the polymer capacity for absorbing water increases with decreasing pH until it completely dissolves at pH 3 – pH4 *(Filipkowska, Jóźwiak, Szymczyk, 2014)*, this has to do with chitosans properties as a base, each monomer is a glucose molecule modified with an amine group. This weak base, (pKa ~6.5) protonates with decreasing pH and the positive charges draws more water molecules into the polymer matrix.

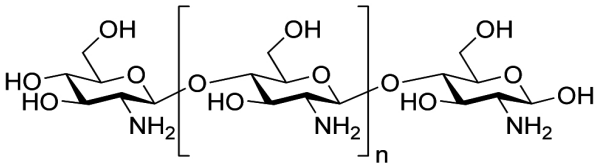

Figure 2.13: Basic structure of chitosan.[6]

Low resistance to diffusion

Ionic species meet little resistance when they diffuse through the widely sized mesh of the swelled matrix, this permeability of the swelled polymer let the water in the swelled phase keep its properties as a solvent.

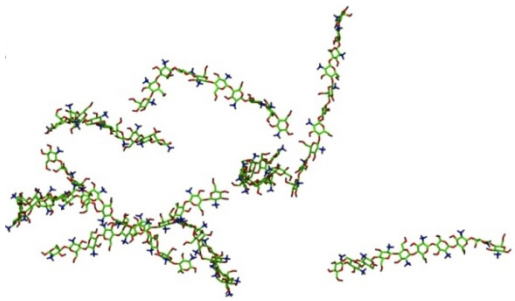

Figure 2.14: Chitosan ball-and-stick illustration, (software 2015)

Mesh size

The average distance between the polymer chains of chitosan swelled with solvent is commonly referred to as *mesh size.* The more water chitosan adsorb, the wider the mesh size, this can have practical implications, since this also mean that any particle that diffuse into the matrix will have less random collisions with the framework of chains if the average mesh between them increases.

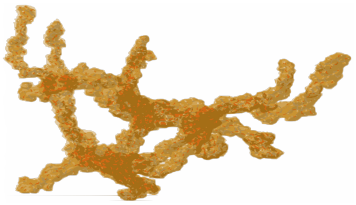

Figure 2.15: Low degree of swelling.

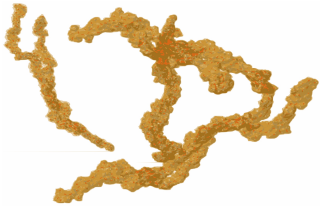

Figure 2.16: Medium swelling.

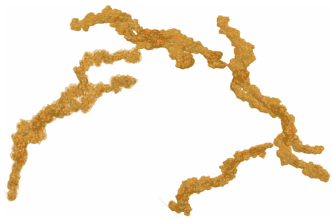

Figure 2.17: High degree of swelling.

Chitosans reactivity

The amine groups of chitosan make the polymer susceptible to several of the same types of reactions as proteins and other polymers with amine groups, this opens up many opportunities when it comes to modifying the polymers properties.[7]

2.4.1 Glutaraldehyde

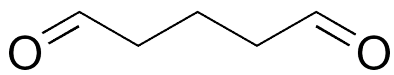

Figure 2.18: Structure of glutaraldehyde. (wikipedia, 2014)

This aldehyde has a linear five carbon chain and can reacts with chitosan to form a covalent bond to a amine group in each end. This cross-linking process increase the polymers structural rigidity without having to sacrifice as much of chitosans hydrophilic properties *(Kildeeva, Perminov, Vladimirov, Nokikov, Mikhailov, 2008)*. This make chitosan useful as a component for making composites, the cross-linking process fuse the chitosan chains which helps to trap anything from macromolecules to larger particles *(Auta, Hameed, 2013)*. In this case the powdered sea shells.

2.5 Adsorption

Both calcium carbonate and chitosan can adsorb phosphate from water, both of these two components will be mixed together to form the basis for a new composite material that will be used to remove low concentrations of phosphate dissolved in water. The mechanism behind how each of these two components adsorb phosphate on their own will be covered separately below.

2.5.1 Adsorption of phosphate onto calcium carbonate

The surface of aragonite and calcite crystals has a polar geometry where the calcium atom acts as a positively charged terminal, or *active site,* that allows for weak electrostatic bonding of negatively charged ions or polar particles with matching properties.

The charged framework on the surface of the crystalline structures of aragonite and calcite will have an affinity for charged particles, though this will vary a lot between different types ionic species.

The difference in this affinity will in most cases result in any initially present anions being replaced by phosphates and to some extent other ionic species. At the start of the process there might be some ionic species present in the shell substrate, the most likely of these will be sodium and chloride which will quickly start to migrate towards the bulk fluid as the phosphates begin to diffuse into the beads.

The adsorption process has so far been suggested to be a surface specific phenomenon since it appears that phosphate is not stored inside the crystal lattice of calcite or aragonite but, rather on the surface of the crystal structures. *(Karageorgiou, Paschalis, Anastassakis, 2006).*

The adsorption of phosphate onto calcium carbonate can be expressed by a simplified model with the following equilibrium equations;

$$[Ca^{[+2]}CO_3^{[-2]}]+[PO_{4(l)}^{-1}] \Leftrightarrow [Ca^{[+2]}CO_3^{[-2]}][HPO_{4(s)}^{-2}] \qquad K=\frac{[Ca^{[+2]}CO_3^{[-2]}]+[PO_{4(l)}^{-1}]}{[Ca^{[+2]}CO_3^{[-2]}][HPO_{4(s)}^{-2}]}$$

Where:

$Ca_{(s)}^{-2}$ *– Calcium terminal* $HPO_{4(aq)}^{-2}$ *– Phosphate carried by solvent*
$CO_{3(s)}^{-2}$ *– Carbonate terminal* $[HPO_{4(s)}^{-2}]$ *– Phosphate bound to exchanger/adsorbent site*

This model assume that that the adsorption mechanism only has one step that happens fast, although research suggest that the adsorption involve more complex mechanisms where the adsorption appears to be a multi-step process. The first stage is fast while the second stage appears to be a slower process which can last over a week *(Millero, Huang, Zhu, Liu and Zhang, 2000).*

When it comes to the difference between calcite and aragonite, it appears that aragonite has a higher adsorption the first 24 hours but, this difference seems to decrease over time *(Millero, Huang, Zhu, Liu and Zhang, 2000).*

There is a number of physical factors that influence the adsorption process, the most significant of these are:

- *pH*

  The common form of phosphate in effluent water is orthophosphoricicciid (H3PO4), which depending on pH can be protonated to forms the following species: H2PO4-1, HPO4-2 and PO4-3. Non-protonated orthophosphoric acid H_3PO_4 has a peak concentration at pH 0, $H_2PO_4^{-1}$ has a peak at approximately ~pH 4.5, HPO_4^{-2} has a peak at approximately ~pH 10 and PO_4^{-3} has a peak at pH 14 *(Liu, Sheng, Dong, Ma, 2011)*, see *figure 2.21*.

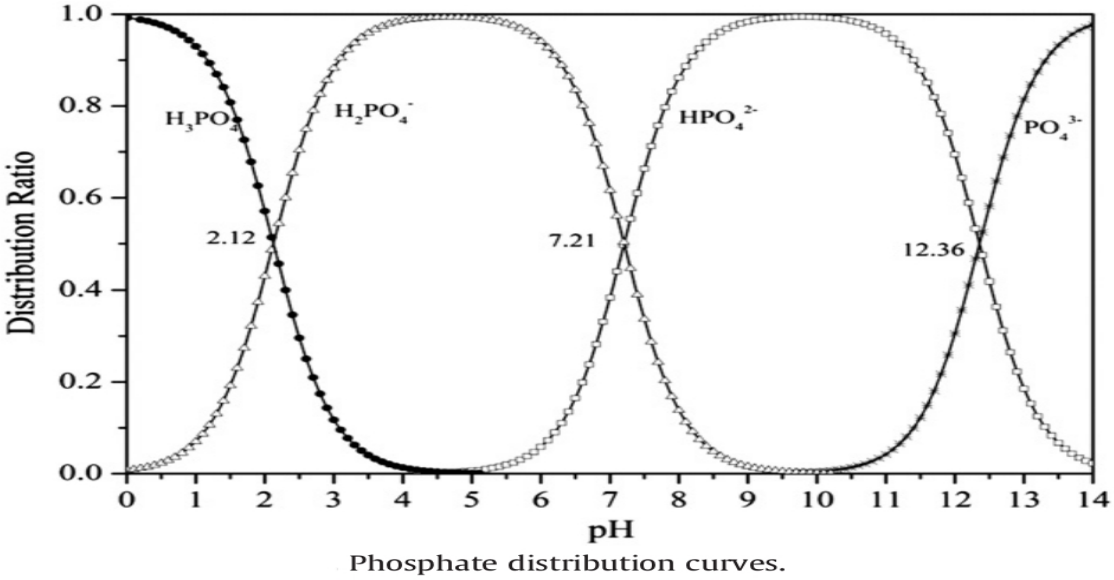

Figure 2.19. ***Courtesy of: Yun Liu, Xia Sheng, Yuanhua Dong, Yijie Ma, "Removal of high-concentration phosphate by calcite: Effect of sulfate and pH" (2011)[13]***

The mineral forms of calcium carbonate has slightly different affinity for the different phosphate species. Previous studies has found:

- For calcite pH has been shown to have an impact on the adsorption of orthophosphate where the adsorption increase from pH7 to pH12 *(Karageorgiou, Paschalis, Anastassakis, 2006)*.

- For aragonite the adsorption increases from pH7.4 and reaches a peak at ~pH8.5 before it decrease for higher pH values *(Millero, Huang, Zhu, Liu and Zhang, 2000)*.

- *Presence of different ionic species*

  Magnesium and calcium, $Mg^{+2,}$ Ca^{+2}

  The presence of Mg^{2+} and Ca^{2+} ions appears to contribute to the adsorption due to a bridging effect *(Millero, Huang, Zhu, Liu and Zhang, 2000)*.

Carbonic acid, HCO_3^-

The same study found that the concentration of HCO_3^- seems to affect the adsorption of phosphate, where higher concentrations of HCO_3^- causes the adsorption to decrease *(Millero, Huang, Zhu, Liu and Zhang, 2000).*

Sulphates, SO_4

The presence SO_4 appears to diminish the bridging effect of Mg^{2+} and Ca^{2+}, the mechanism behind this appear to be formation of $MgSO_4$ and $CaSO_4$ complexes as well as competitive adsorption onto the surface of calcite and aragonite *(Millero, Huang, Zhu, Liu and Zhang, 2000)*.

Low concentrations of sulphate (SO_4) in acidic conditions has been demonstrated to increase the adsorption of phosphate while higher concentrations inhibit the adsorption *(*Liu, Sheng, Dong, Ma, 2011).

At high pH the adsorption increased with increasing concentrations of sulphate, though this might be because of increased solubility of calcite in the presence of sulphate *(*Liu, Sheng, Dong, Ma, 2011).

- *Temperature*

  Temperature has previously been demonstrated to be a factor for the adsorption of phosphate onto calcite and aragonite, where an increase temperature lead to an increase in equilibrium adsorption *(Millero, Huang, Zhu, Liu and Zhang, 2000).*

- *Adsorption of contaminants*

  Calcium and aragonite has an affinity for charged particles which in theory is not limited to phosphate, although there are not likely to be many contaminants that has a higher affinity than phosphate.

2.6 Chitosans capacity for adsorbing of phosphate

pH and Amine groups, ($R–NH_2$)

The amine groups along the polymer chains of chitosan each act as weak bases, $pK_a \sim 6.5$ [6]. A portion of these amine groups will protonate depending on the acidity of the surrounding water, these groups, $R–NH_3^{+1}$, will then be positively charged and able to attract negatively charged ionic species, like phosphates.

Its may seems intuitive that if these amine groups are also used for the cross-linking process, then less of these should be available to adsorb phosphate if a large portion of cross-linking is used. Fortunately the effect of cross-linking on adsorption of phosphate has been confirmed to not block the active sites of chitosan, in fact the cross-linked chitosan was found to have a higher adsorption capacity *(Filipkowska, Jóźwiak, Szymczyk, 2014)*.

Neutral conditions, pH7

Chitosan has previously been found to adsorb phosphate at a rate of 4.5 mg/g [PO4/chitosan] at pH7, while for the same conditions ,chitosan cross-linked with glutaraldehyde had a capacity found to be slightly higher at approximately 5 mg/g *(Filipkowska, Jóźwiak, Szymczyk, 2014).*

Optimal pH for adsorption of phosphate

For non-cross-linked chitosan the optimal pH for adsorbing phosphate has previously been found to be pH 4, with a maximum adsorption capacity of approximately 44.38 mg/g, although it it important keep in mind that non-modified chitosan dissolve completely below pH4 *(Filipkowska, Jóźwiak, Szymczyk, 2014).*

For cross-linked chitosan however, the optimal pH for phosphate adsorption has similarly been found to be about pH 3, with a maximum capacity of 108.24 mg/g for chitosan cross-linked with glutaraldehyde *(Filipkowska, Jóźwiak, Szymczyk, 2014).*

2.6.1 About selectivity

For both calcium carbonate and chitosan the general principle is that ionic species that attach onto charged sites will be replaced if it has lower affinity for the adsorbent material than the other particles in the fluid, this property is referred to as the charged frameworks *selectivity*.

Both calcium carbonate and chitosan has generally a higher affinity for phosphate than other ionic species present in the effluent water, although in theory there can be species that compete with phosphate for adsorption *(*Liu, Sheng, Dong, Ma, 2011).

The main mechanisms behind the differences in selectivity explained in the following section is based on the explanation given by Nasef and Ujang, (2012, p.18):

- Electrostatic interaction between counter ions and the active sites on the charged surface framework depends on valence of counter ion as well as the size of ionic radii on both charges.
- The molecular geometry or steric effects of framework and counter ion.
- Interactions between other ions present, formation of double layers and other weaker electrostatic complexes.
- The narrow pores or mesh size of a polymer matrix may sterically hinder larger particles from reaching active sites.

2.6.2 Cross-linking of chitosan with glutaraldehyde

The explanation of the mechanism behind the reaction between chitosan and glutaraldehyde given below is based on the article by Kildeeva, Perminov, Vladimirov, Nokikov and Mikhailov (2008).

Glutaraldehyde reacts readily with the amine groups of chitosan under alkaline conditions. Glutaraldehyde is a linear saturated five carbon chain with one formyl group in each end, each formyl group can form imine linkages with a nearby amine group and effectively cross-link two polymer chains.

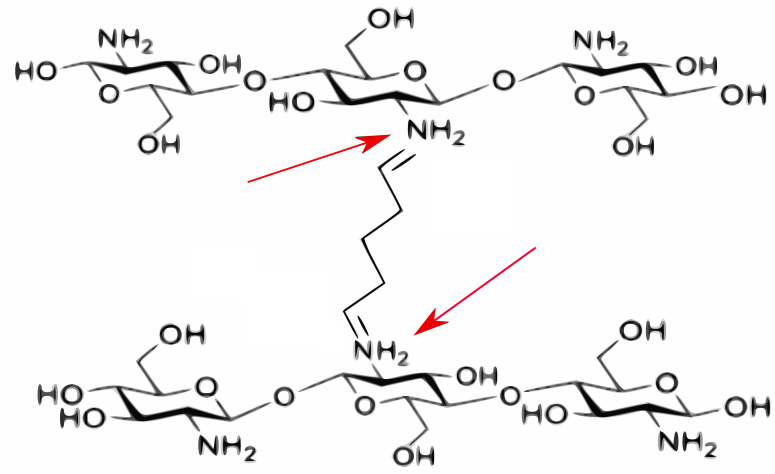

Figure 2.20. Cross-linked *chitosan.*

As the reaction proceed the resulting random cross-linking of the chains result in a matrix that grow denser since the average *mesh size*, continue to decrease *(Kildeeva, Perminov, Vladimirov, Nokikov, Mikhailov, 2008)*. This will affect several characteristics of the final product, these are:

- *Capacity for swelling*

At pH 7 and 25^{0}C, non-cross-linked chitosan has previously been found to have a swelling ratio of ~650%, while chitosan with 8% molar ratio of cross-linking with glutaraldehyde had a swelling ratio of ~140% and 16% cross-linking was found to reduce the swelling further to about 80% (Rohindra, Nand, Khurma, 2004).

Resistance to diffusion

As the mesh size decreases, migrating molecules will need more time to diffuse through the matrix. Since diffusion happens through random collisions, larger particles will collide more frequently with the chains in the mesh, this result in a slower rate of diffusion as size increases until the rate is too low to be of any use. This may in some cases also work as a desired property for cutting off diffusion of larger unwanted particles.

It is important to remember that this effect will largely depend on the size of the diffusing particle as well as the thickness of the polymer layer it diffuses through. For small particles like phosphate, the reduction in swelling volume may also reduce the diffusion resistance, which means that the end result of higher cross-linking may result in overall lower diffusion resistance *(see equation 2.7.5.6, section 2.7.5)*.

2.7 Thermodynamics

2.7.1 Distribution coefficient

Section 2.7.1 – 2.7.2 is based on ch.1, p.17 by Nasef and Ujang and ch. 4 by Inglezakis and Zorpas from the book "Ion Exchange Technology I: Theory and Materials" (2012):

The adsorbent materials capacity for removing specific ionic species from a solvent can be measured by finding the distribution coefficient, K_d

It is an empiric quantity defined by the ratio of the concentration of an ionic species in the solid phase to the concentration in the liquid phase. It is commonly determined by reassuming the difference in concentration from start to finish in a batch-wise test run. The distribution coefficient is calculated empirically from the following formula:

$$K_d = \frac{(C_i - C_f)}{C_i} \cdot \frac{V_s}{m_e}$$

C_i – *Initial concentration in solution*
C_f – *Final concentration in solution*
m_e – *Mass of adsorbent used*
V_s – *Volume of solution*

Like pointed out earlier, $\boldsymbol{K_d}$ can only be reasonably accurate for the specific conditions in the test environment. When scaling for industrial applications like a setup with continuous flow, $\boldsymbol{K_d}$ will have to be determined for a span of likely variations in physical parameters. For efficient large scale removal of ionic species, natural variations in physical parameters and concentrations will need to be monitored in order to adjust flow or mass of exchanger to meet the resulting variations in ionic driving force.

2.7.2 Relation to Gibbs free energy

The value of the empirically found adsorption constant, $\boldsymbol{K_d}$ relate to the systems temperature through *Gibbs free energy* of adsorption *(equation 2.7.2)*, this thermodynamic potential can be considered the *ionic driving force* given by:

$$\Delta G^0_{adsorbtion} = -RT \cdot \ln K_d$$ Equation 2.7.2, w*here:*

$\boldsymbol{\Delta G^0}$ – *Standard change of free energy, [J]*

T – *Absolute temperature, in Kelvins [K].*

R – *Universal gas* $[8.314 \frac{J}{mol\,K}]$ *constant,*

Phosphate will reduce it's thermodynamic potential when it attaches to the active site on the mineral, the net change in Gibbs free energy will be negative. This change in energy is the difference between *equation 2.7.2 and equation 2.7.3* where the latter represents *Gibbs free energy of solvation* given by:

$$\Delta G^0_{solution} = -RT \cdot \ln K_s$$ *Equation 2.7.3:* $\boldsymbol{K_s}$ *represents the temperature dependent solvation constant for phosphate in water.*

the This change in energy state is large enough to result in an ionic driving force can be expected to make the adsorption process happen very quick *(M.M. Nasef and Z. Ujang, 2012, p.19).*

2.7.3 Diffusion, mass transfer and kinetics

Section 2.7.3 is partially based on Ch.9: adsorption, ion exchange from book "Thermal Separation Technology: Principles and methods" by A. Mersmann (2011).

The rate of adsorption can be expressed by reaction kinetics. For industrial scaling of ionic adsorbent process' the resistance to mass transfer of ionic species will vary in both phases as the adsorbent approach saturation. The design and operation of the process will depend highly on how to find a balance between mass transfer and operational expenses.
Mass transfer will decide the scale of adsorption columns, rate of liquid flow, pipe diameters and power consumption.

Kinetics are affected by operation temperature, the nature of the adsorbent material, differences in concentration between liquid and solid phase, structure of adsorbent beads, rate of liquid flow, the type of liquid and competing ionic species.

The ion adsorption process taking place between adsorbent bead and the surrounding solution can be divided into a number of distinct steps, each of them can be the rate limiting step, the «bottleneck» of the ionic mass transfer *(A. Mersmann, 2011).*

For a composite bead made of chitosan and shell particles, *figure 2.24*, we have:

1. *Diffusion of ions from the bulk solution surrounding the bead, to the fluid surface film coating the bead.*

   This is the part of the fluid that has the more or less the same concentration as fluid flowing freely in the gaps between the beads. In this portion of he fluid the concentration decrease with the height of the adsorption column.

2. *Diffusion through the beads fluid surface film.*

   A thin film of fluid coating the bead surface has no velocity, diffusion through this layer happens through passive diffusion since there is no currents.

3. *Diffusion through the layers of swelled polymer matrix.*

   Rate of diffusion through swelled polymer is lower than for the bulk fluid, although for smaller particles this is close to passive diffusion. The diffusion rate decrease rapidly with the effective thickness of this layer. Shape and size of the beads can greatly reduce this diffusion resistance.

4. *Electrostatic attachment to a charged site on calcite/aragonite.*

   Each time a phosphate particle collide with a charged site on the crystal surface it has a certain chance of attaching, depending on physical conditions this can be close to permanently.

5. *Displacement of competing ionic species bond to charged sites.*

Other anionic particles can also attach to charged sites, although since the selectivity is usually lower they are much more easily knocked out of position and will be displaced by phosphate in time. The overall chance for a phosphate molecule to displace and then attach to the site is slightly lower than for a vacant site. This step can normally be expected to be negligible, in cases it does have an impact this will usually result in somewhat delayed saturation of phosphate and also a small ratio of contaminates.

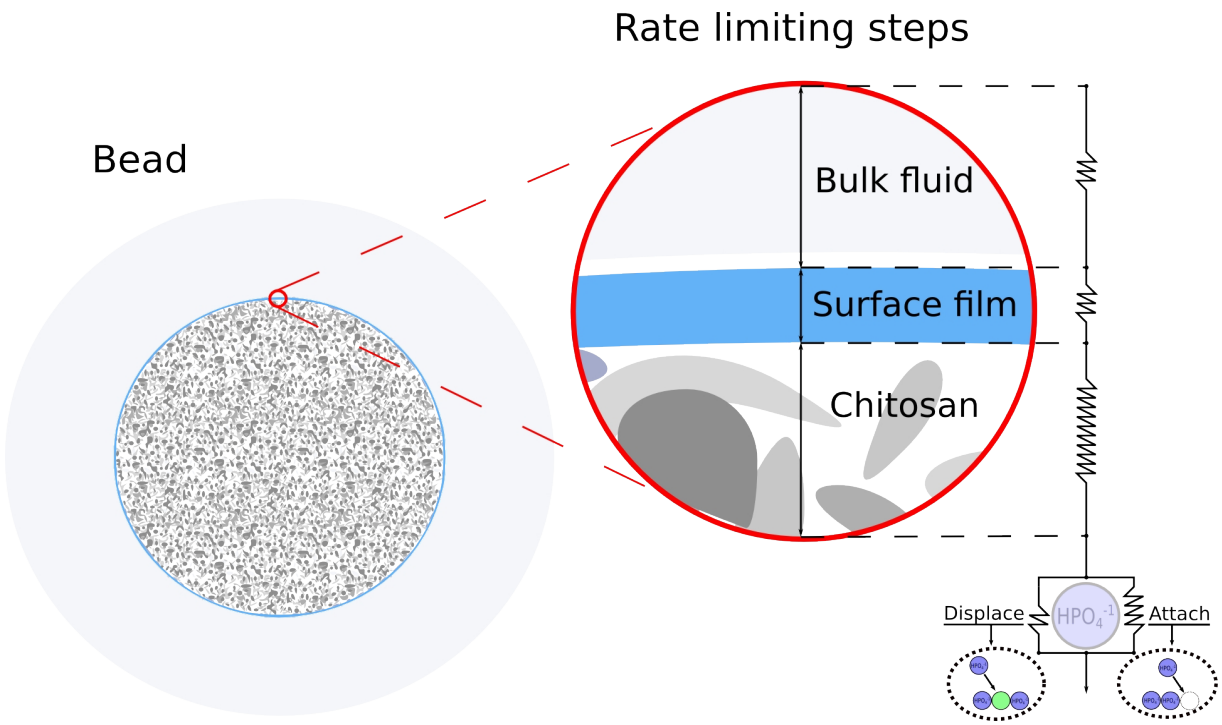

Figure 2.21: Illustration of the possible rate limiting steps in the adsorption process.

Notes: Size of resistance symbol is meant to illustrate the proportions between the different steps involving resistance to diffusion.

Step 1: *Passive diffusion in the fluid, stationary fluid and fluid with velocity will have an impact on this step.*

Step 2: *The layer of stationary fluid coating the bead, this step has only passive diffusion.*

Step 3: *Represent the phase of swollen polymer that the active species (phosphate) only can diffuse by passive diffusion. The chemical potential is the main driving force behind this diffusion, this is common to be the rate-limiting step.*

Step 4: *Displacement resistance is often negligible, this step is likely to be affected by pH.*

Step 5: *Active species attaches to an active site, the resistance to attachment is lower with increasing affinity between active site and species. This step is influenced by pH like mentioned in section 2.5.1.*

2.7.5 Mass transfer from a mathematical view

Due to limitations in this project the following theory is meant to explain how the mathematical principles behind diffusion, predicts in broad terms how physical parameters such as thickness of the material used in adsorption beads, more or less directly affect how fast the mass transfer will carry out. Section 2.7.5 is based on ch. 4, p.126 by Inglezakis and Zorpas from the book "Ion Exchange Technology I: Theory and Materials" (2012):

Fick's first law

This expression relates the diffusive flux, the mass transfer to the concentration field by the assumption that the mass flux goes from regions of high concentration to the regions of low concentrations with a magnitude that is proportional to the concentration gradient. The mass flux ***J*** of species ***i***, is expressed as*:*

$$J_i = -D \cdot grad(C_i) = -D \cdot \nabla C_i \quad \textbf{2.7.5.1}$$

Where C_i is the concentration and D is the diffusion coefficient, the minus sign signifies that the diffusion occurs in opposite direction to that of increasing concentrations. In dilute concentrations, the diffusion coefficient can be considered constant for most practical applications. *(In ion exchange system an electric field is developed and the flux related to electric potential could be added.)*

When there is an exchange of counter ions ***A*** in a solid phase and a counter ions ***B*** in liquid, a common expression is the *Nerst-Planck equation*:

$$J_i = -D_i \cdot C_i - u_i \cdot z_i \cdot C_i \nabla \varphi = -D_i \cdot \left(\nabla C_i - \frac{z_i \cdot C_i \cdot F}{R \cdot T} \cdot \nabla \varphi \right) \quad \textbf{2.7.5.2}$$

Where:

***u**$_i$* *= Electrochemical mobility*
φ *= Electric potential*
z *= Ion exchange*
T *= Temperature*
R *= Gas constant*
F *= Faraday constant*

When taking into account that the system needs to electrically neutral and that there wont be any electric current, the equation is reduced to:

$$J_i = -D_{AB} \cdot \nabla C_i \quad \textbf{\textit{Equation [2.7.5.3]}} \textit{ where } \textbf{\textit{D}}_{\textbf{\textit{AB}}} \textit{ is given by:}$$

$$D_{AB} = \frac{D_A \cdot D_B \cdot (z^2{}_A \cdot C_A + z^2{}_B \cdot C_B)}{z^2{}_A \cdot C_A \cdot D_A + z^2{}_B \cdot C_B \cdot D_B} \quad \textbf{Equation [2.7.5.4]:} \textit{ Subscript } \textbf{\textit{A}} \textit{ and } \textbf{\textit{B}} \textit{ represents counter ion A and B.}$$

D**$_{AB}$* is called the inter-diffusion coefficient and depends on the individual diffusion coefficients of counter ions ***A and ***B*** as well as the local concentration of both species which leads to the radial position and time. The effect of the electric field is expressed by the variant inter-diffusion coefficient.

If the two counter ions have equal mobility (or if the process is more of an adsorption process than ion exchange), then ***D**$_{AB}$* becomes equal to the self-diffusion coefficient of each ion (or single ion) and the equation $J_i = -D_{AB} \cdot \nabla C_i$ reduces back to $J_i = -D \cdot \nabla C_i$

To simplify things further, an average constant value could be used under many practical applications. When dealing with a system consisting of a solid phase having a pore structure filled with liquid, as is the case of chitosan where the polymer represents a solid matrix, then we can consider it to be a single quasi-homogeneous phase. In this case the diffusion constant that we measure is more or less an average value for the mass transport taking place.

To express the time dependence of local concentration we get the following version of *Fick's second law*:

$$\frac{\partial C_i}{\partial t} = -(J_i) = D \cdot \nabla^2 C_i \qquad \textbf{\textit{Equation 2.7.5.5}}$$

"Fick's second law is derived from the first law and the mass balance predicts how how diffusion causes the concentration to change with time" (wikipedia, 2014).

By combining *Fick's first and second law* and expressing the mass transfer process in spherical coordinates, we get the following time dependent diffusion equations for spherical particles:

$$\frac{\partial C_i}{\partial t} = D_s \cdot \left(\frac{\partial^2 C_i}{\partial r^2} + \frac{2}{r} \cdot \frac{\partial C_i}{\partial r} \right) \quad \textbf{Equation 2.7.5.6}$$

If we relate this equation to the amount of cross-linking *(section 2.6.2)*, we can see that higher crosslingmay increase the value of $\boldsymbol{D_s}$ while at the same time a reduction in swelling volume will lower the value of the distance $\partial \boldsymbol{r}$. If the beads are sufficiently small it may be more favorable with higher amount of cross-linking if the reduction in $\boldsymbol{D_s}$ turns out to be low compared to the reduced diffusion resistance gained by lowering $\partial \boldsymbol{r}$ *(Inglezakis and Zorpas, 2012, p.126).*

2.8 *Definitions*

Screening experiments

A definition of screening experiments can be found in the book "e-Handbook of Engineering Statistics, NIST/SEMATECH, (2014)", which states:

"The term 'Screening Design' refers to an experimental plan that is intended to find the few significant factors from a list of many potential ones. Alternatively, we refer to a design as a screening design if its primary purpose is to identify significant main effects, rather than interaction effects, the latter being assumed an order of magnitude less important."

3.0 Method and Materials

Table of materials				
Name	**Formula**	**Notes**	**Supplier**	**Experiment reference**
Water	*H_2O, purity: tap water*	trace amounts of minerals	Oppegård vannverk	3.2, 3.3, 3.4.3, 3.5.2, 3.6.0
Water	*H_2O, Non-purified*	Effluent, main phosphate source	Fiskelabben, nmbu	3.4, 3.5
Glutaraldehyde	*$CH_2(CH_2CHO)_2$*	C: 5%, 0.5%, 0.1%	Sigma-Aldrich	3.3.6, table 3.5.1
Sodium hydroxide	HCl	C: non specific	Jotun	3.3.2
Hydrochloric acid	NaOH	C: non specific	Jotun	3.3.2
Phosphoric acid	H_3PO_4	C: 3.51 mg/l, 3.44 mg/l	Sigma-Aldrich	3.4.3, 3.5.2
Shell substrate	Natural, $CaCO_3$ mineral form: calcite, aragonite	C: $CaCO_3$ > 98%, ratio of calcite/aragonite not specified	Franzefoss Miljøkalk AS	*3.1, 3.2, 3.3, 3.4, 3.5, 3.6*
Chitosan	β-(1-4)-linked D-glucosamine, ($_n[C_6H_{13}NO_5]$)	~ 80% deacetylated, *KitoFlokk*	Chitosan Norge	*3.3, 3.5, 3.6*

Table of equipment				
Name	**Type**	**Notes/model**	**Supplier**	**Experiment reference**
Phosphate test reagent	Test Equipment		Merc	3.4, 3.5
Spectroquant 60	Test Equipment		Merc	3.4, 3.5
Beaker	600ml	Glass	Schott Duran	3.3, 3.6.0
Erlend meyer flask	850ml	Glass	Schott Duran	3.3.6, 3.5.3
Magnetic stirrer + large rod	Test Equipment	Compact HP 1	Variomag	3.6.0
Electronic pH meter	Test Equipment	Handy	Oxyguard	3.4.2
Weight, 0.000g	Test Equipment	AG204	Deltarange	3.2, 3.3, 3.4, 3.5, 3.6.0
Stopwatch	Test Equipment			3.5.3
Adsorbtion column, 425mm	Test Equipment	Plastic	Custom	3.5.4
Tub, large		Plastic		3.3
Bottle 100ml		Plastic	Sarstedt	3.4.1
Bottle 250ml		Glass	Schott Duran	3.4.3
Bottle 500ml		Glass	Schott Duran	3.4.2, 3.5.2
Mill, cutting		1mm sieve pass	Fritsch P-19	3.1.2
Syringe filter	Test Equipment		Sigma-Aldrich	3.4, 3.5
Sieving apparatus			Retsch	3.1.3
Sieve 1 mm	Sieve disc		Retsch	3.1.3
Sieve 0.8mm	Sieve disc		Retsch	3.1.3
Sieve 0.6mm	Sieve disc		Retsch	3.1.3
Sieve 0.5mm	Sieve disc		Retsch	3.1.3
Sieve 0.4mm	Sieve disc		Retsch	3.1.3
Sieve 0.3mm	Sieve disc		Retsch	3.1.3
Sieve 0.2mm	Sieve disc		Retsch	3.1.3

3.1 Pretreatment of materials

3.1.1 Drying

The raw shell substrate was wet when received and had to be dried, it was then spread out to a thin layer on plates and left to dry at room temperature until it reached a stable moisture level.

A 50g sample of the dry substrate was subjected to a further drying process at 80^{o}C and was found to have less than one percent reduction in weight. From this it was assumed that the moisture content in the substrate dried at room temperature was unlikely to have more than a few percent moisture. The total offset in the substrates dry weight was considered likely to be somewhere between one to five percent at most.

3.1.2 Milling

The shell substrate was milled by a cutting mill fitted with a sieve that had a pass of one millimeter. In the milling process it was apparent that a high amount of very fine dust was generated which could be considered an indication of low moisture content, the milling generated an considerable amount of heat which could potentially have contributed to further lowering of the substrates moisture content.

3.1.3 Sieving

After milling the substrate was dry sieved into a set of fractions spanning from 1 – 0.1mm, table. 3.1.1. The process of dry sieving produce a reasonable accurate distribution of the average particle diameters within each fraction, although there is a few factors that limits to the accuracy of maximum and minimum particle size.

Generation of static charges
The particles have a tendency to generate static charges during the sieving process. This causes them to lump together, these small clusters will not pass the sieve easily since they tend to float on the electric fields generated in the sieving process.

Friction
Calcium carbonate minerals are brittle by nature and will to some extent break up into smaller particles as they are rub against each other at the high frequency of the sieving process. This continuous production of fine particles makes them difficult to avoid being present in each separated fraction.

Table 3.1.1: List of sieve diameters

Sive nr.	1	2	3	4	5	6	7	8	9
Diameter	1mm	0.8mm	0.6mm	0.5mm	0.4mm	0.3mm	0.2mm	0.1mm	<0.1mm

3.2 Analysis of particle size

After sieving each fraction was analyzed with a *Mastersizer* optical instrument, the first two fractions was too coarse for the instrument to handle and so these was left out of the analysis. Samples were between 1-3g and was performed with a water as a dispersion medium.

3.3 Bead production

3.3.1 Introduction

To get a better understanding of what affects the performance of these beads, I chose to focus on how finely milled shell substrate would affect the end products capacity for adsorbing phosphate. It seemed reasonable to expect the mineral to be most predicable component and the easiest to understand, this project was limited to experimental screening to see if this type of composite would provide benefits compared to using either component preparatively.

Stages in production

3.3.2 First stage, preparation of polymer

In order to mix chitosan and shell substrate into a consistency where the two components are dispersed evenly into a fine paste, the first step will be to have the polymer adsorb water and swell into a large volume. This will decrease the polymers mass density and make it soft and easy to mix with the dry shell substrate.

Chitosan was first mixed with water *(figure 3.3.2a)*, then diluted hydrochloric acid was gradually added until all the polymer was dissolved *(figure 3.3.2b)**. Then the polymer solution was diluted further with water, before sodium hydroxide was added to make the polymer separate from the dissolved phase *(figure 3.3.2c)*. The polymer start to form small suspended particles that flocculate and sediment to the bottom of the tub *(figure 3.3.2d)*. The suspension is then left to settle before the layer of clear water at the top is removed and the sediments are drained in paper filters.

**Note: The amount and concentration of hydrochloric acid needed to dissolve chitosan will depend on temperature, degree of deacetylation and other factors. In this experiment the amount and concentration of hydrochloric acid used was not specified, although chitosan dissolves completely between pH3 – pH4.5, chitosan will start to sediment efficiently at pH7 to pH8. Solutions with dissolved polymer can be problematic to measure with a pH meter due to coating of the electrode. The only impact of the amount of acid used would be how much sodium hydroxide would be needed for neutralization. The resulting bead material would at any rate need to be washed of sodium chloride, sodium hydroxide and other bi-products in the production process.*

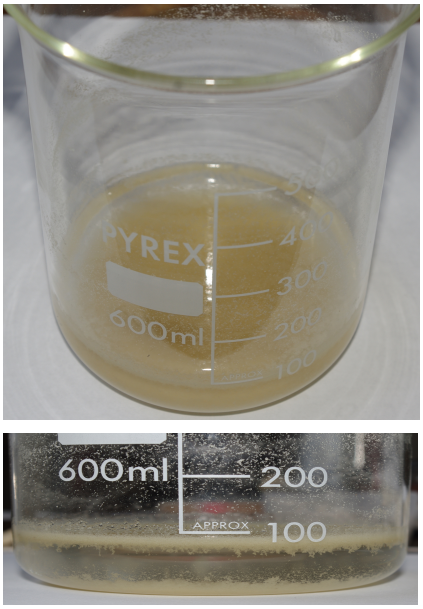

Figure 3.3.2a: Raw chitosan in water

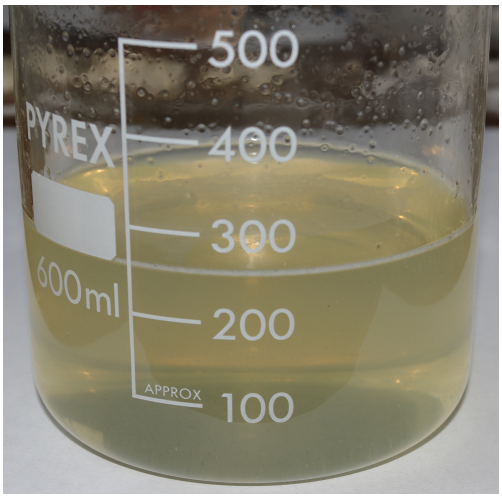

Figure 3.3.2b: Dissolved chitosan, after adding HCl

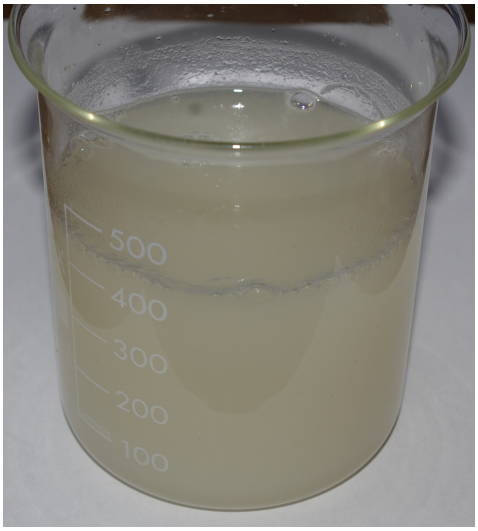

Figure 3.3.2c: Phase separation after adding NaOH

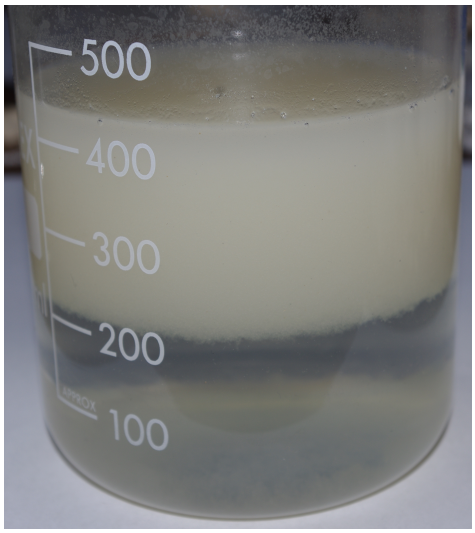

Figure 3.3.2d: flocculation, in this case the chitosan float as a result of air bubbles, after some stirring the chitosan phase will settle at the bottom.

3.3.3 Second stage, mixing

The dry shell substrate and the wet chitosan is mixed thoroughly and molded into long thin lines on a plate to prepare them for drying.

3.3.4 Third stage, drying

The molded lines of raw bead material is dried in open air until they reach a hard and brittle texture before they are crudely broken up into smaller units.

3.3.5 Fourth stage, leaching

The beads are soaked in water to leach out any residual salt left by the sodium hydroxide and hydrochloric acid.

3.3.6 Fifth stage, cross-linking reaction

The wet rinsed beads are submerged in a solution of glutaraldehyde to initiate a cross-linking reaction, the time of exposure will determined the amount of cross-linking in the resulting product. Afterwards the beads are again dried for storage.

3.3.7 Sixth stage, finding a useful ratio of chitosan and powder

The first goal was to find a decent ratio between chitosan and mineral powder that would be well within the safe range for a structurally rigid product.

The first step was to try to produce tiny quantities of a set of different mixtures with 25, 30 and 35 percent chitosan. After they were dried and then allowed to swell in water without the use of cross-linking agent, the beads with 30 percent chitosan seemed to have reasonable flexibility without being too brittle, the chitosan ratio was then increased to 32 percent to make sure the next batch would be a bit more structurally rigid.

All mixes were reasonably stable in still water, though to be sure the beads would survive some degree of wear and tear by rubbing against each other, the one at 32% was chosen as a safe starting platform. After all, finding the ideal composition for mechanical durability was not the goal of this stage.

3.4 Adsorption with shell substrate

Substrate made from milled and sieved sea shells

Each sample of shell milled sea shells was obtained by sieving like explained in the methods chapter. The diameter of each sieve pass is listed in table 3.1.1.

This experiment build on the results found from the analysis of particle size distribution, where the main objective is to examine whether the shell substrate has a capacity for adsorbing phosphate that scale with its estimated value for specific surface.

Explanation

Each sample is more finely milled than the previous which gives is more specific surface area [m^2/g]. More surface area result in a higher density of active calcium sites that can bind phosphate molecules.

Changes in capacity

The most simple way to define capacity for the substrate is to consider the quantity of phosphate that is adsorbed for each unit mass of adsorptive substrate, in this case we have the ratio of milligrams of phosphate that is adsorbed for every gram of shell substrate.

3.4.1 Series one, adsorption with effluent water, sample 1–6

Setup

This experiment was performed by adding 200mg of milled shell substrate to 100ml of effluent water, this was done with sample 1-6, table 3.4.1. The sample was shaken vigorously, left to rest for 5 minutes afterwards before taking a liquid sample of 5ml, table 3.4.2. The 5ml sample was filtered through a syringe filter to remove any suspended particles before it was analyzed for phosphate content with a photometric test kit from Merck.

Table 3.4.1

Sample	1	2	3	4	5	6
Sieve pass	1mm	0.8mm	0.6mm	0.5mm	0.4mm	0.3mm

Table 3.4.2

Start concentration	Substrate amount	Sample volume	Exposure time
0.18 mg/l	200mg	100ml	5min

Errors and noise

Samples were done at least twice. For the finer milled samples, a syringe filter had to be used in order to remove suspended particles before phosphate measurements could be done. These filters did give a contaminated sample at one occasion.

Samples were stored in air proof 100ml sample containers to keep the substrate dry. If exposed to humid air they could in theory adsorb minor amounts of water, and the amount weighted for each sample could be off by a few percent.

Rate of adsorption

Two control samples, from both 1mm and 0.1mm sieve was tested after 30 minutes and compared to the results from 5 minutes of exposure. No difference were found between samples of five and 30 minutes of exposure.

Start concentration

The first set of samples was done with effluent water at a start concentration of 0,18mg/l phosphate, table 3.4.2.

3.4.2 Series two, the influence of pH, sample 8–9

Setup

In this set of samples the purpose was to test whether pH would have any significant influence on the shell substrates capacity for adsorbing phosphate. Only sample 8-9 of shell substrate was used in this experiment, table 3.4..3

The samples was done with 400ml test tubes and 100mg of powder, table 3.4.4. The reason for this was because samples done with a lower fluid volume and more substrate in the previous series, where the samples consisted of 100ml and 200mg had phosphate concentrations below the minimum threshold concentration threshold of 0,05mg/L. This was the lowest concentration the instrument could detect.

Table 3.4.3

Sample	8	9
Sieve pass	0.1mm	<0.1mm

Table 3.4.4

Start concentration	Substrate amount	Sample volume	Exposure time
0.15 mg/l	100mg	400ml	5min

Start concentration

The start concentration for the effluent water was 0.15mg/l phosphate for this set of samples, table 3.3.2. Only fresh sample water was used.

pH

For series two sample water had pH7.35 and was adjusted to pH6, pH8 and pH9 with either hydrochloric acid or sodium hydroxide.

3.4.3 Series three, adsorption with diluted phosphoric acid, sample 9

The purpose of this experiment was to see whether there would be any difference between effluent water and purified water containing phosphoric acid.

In this experiment 300mg of the finest fraction of milled shell substrate, table 3.4.5, was added to a 200ml solution of 3.44mg/l of phosphoric acid, table 3.4.6

A sample of 2.5ml was taken for phosphate measurement then diluted by 50 percent before adding reactants, the measured concentration was then corrected by a dilution factor of 2.0, this was done to avoid the potential drop in accuracy that may occur with high and low sample concentrations.

Table 3.4.5

Sample	9
Sieve pass	<0.1mm

Table 3.4.6

Start concentration	Substrate amount	Sample volume	Exposure time
3.44 mg/l	300mg	200ml	15min

3.5 Adsorption with bead material

3.5.1 Batch adsorption, sample 1-3

Method and preparation of beads

In these experiments the purpose was to test the capacity for a sample batch of beads as well as to see if the degree of cross-linking would affect the capacity and to some extent also the rate of adsorption. The bead materials reduction in swelled volume that results of cross-linking, might not be as apparent visually since chitosan only make up about one third of the material. The differences in volume between beads with different amount of cross-linking may even more difficult to spot.

Three samples each of 3g of beads were treated with different amounts of cross-linking agent to test weather cross-linking would have any significant impact on the capacity. The beads used for this experiment had a composition of 32 percent chitosan and 68 percent powdered shell material.

The bead were prepared in the following order:

- Bead sample 1, table 3.5.1, was prepared by exposing 3g of bead material in 300ml solution of 5% glutaraldehyde so that it would have a high degree of cross-linking, at least of what was achievable under given conditions for the reaction.

The change in structural properties was easily observable in how the consistency went from soft and brittle, to almost resemble natural polymers with both rigid and elastic properties like natural rubber. After the treatment the cross-linked beads both resist compression and go back to the original shape after a significant degree of deformation.

- Bead sample 2, was taken from a batch where 300g of beads were first allowed to swell then submerged in 400ml solution with 0.5% glutaraldehyde, for 30 minutes, table 3.5.1.

The subjective changes in the beads was visible in the form of more structural strength and elastic properties, although they were still nowhere near as tough as the sample treated with a heavy degree of cross-linking.

- Bead sample 3, was prepared by exposing 3g of swollen bead material in 200ml of water with a concentration of 0.1% glutaraldehyde for 15 minutes, table 3.5.1.

Even with a relatively minor amount of reactant the material still gained a surprising change in physical properties, when handled in was apparent that the beads had become far more elastic and structurally rigid than expected.

Table 3.5.1

Sample	Chitosan, ratio	Shell substrate, ratio	Amount, bead material	Crosslinking, reaction time	Glutaraldehyde
1	32%	68%	3g	180min	5%
2	32%	68%	3g	30min	0.5%
3	32%	68%	3g	15min	0.1%

Setup

A simplified setup was used consisting only of a volumetric flask with a capacity of 200ml. The flask was filled with effluent water where the phosphate content had been determinate with a photometric test kit from Merck. After 72 hours the phosphate content was tested again then replaced with fresh water that had a high phosphate content. The combined differences in phosphate content for each cycle of 72 hours was used to determine the total adsorption that had taken place.

When there was no more observable difference in phosphate content after 96 hours the beads was assumed to have reached a saturation equilibrium.

3.5.2 Adsorption test with diluted phosphoric acid, sample 3

Setup

In this experiment the goal was to investigate how the bead material would behave in an environment free of microbes, contaminants, particles and other factors that could affect the adsorptive performance.

A 400ml solution was prepared with a concentration of 3.51mg/l phosphoric acid, 1g of bead material was added, table 3.5.2. The bead material had a moderate amount of cross-linking similar to sample 3 in table 3.5.1.

Table 3.5.2

Start concentration	Substrate amount	Sample volume
3.51 mg/l	1g	400ml

3.5.3 Rate of adsorption in batch, sample 2

Method and setup

In this experiment the purpose was to test the rate of adsorption in a batch setup. This was done by exposing 50grams of swelled beads to 800ml of effluent water, table 3.5.4. The beads were exposed to effluent water in an Erlenmeyer flask with continuous stirring. A 5ml sample was taken every two minutes for the first 12 minutes to see if there was any fast acting changes, the next sample was taken after 56 minutes, then after 69 minutes, the final sample after 89 minutes, table 3.5.3.

Table 3.5.3

Sample	1	2	3	4	5	6	7	8	9	10	11
Time	0	2min	4min	6min	8min	10min	12min	14min	56min	69min	89min

Goal

Batch has different conditions than a setup with continuous flow because the water surrounding the adsorption material will eventually reach an equilibrium between the concentrations inside the material and outside in the surrounding bulk fluid. With continuous flow we can expect the difference in concentration will be larger between the two phases and thus the ionic driving force, the chemical potential will also be a stronger factor in the interactions between the solid

and the liquid phases. The difference between a continuous flow and a batch setup can give indications to whether the process has a mechanism involving exchange ionic species or if it is more of a direct acting adsorption process.

Like previously mentioned at page [?], an ion change process tend to favor conditions with continuous flow rather than more stationary liquid in a batch.

Materials
For this experiment beads had the same composition as previously with 32% chitosan and 68% shell powder. The beads had a degree of cross-linking similar to sample number 2, table 3.5.1.

Table 3.5.4

Start concentration	Substrate amount	Sample volume
0.25 mg/l	50g	800ml

3.5.4 Adsorption in a column with continuous flow, sample 2

In this experiment a cylindrical column of transparent plastic was filled with beads and a small rate of water was run trough. To standardize the effective thickness of the beads they were crudely broken up into smaller pieces that had a controlled maximum thickness. From this an average thickness and volume was estimated for the average bead in the column.

The beads in this mixture had a composition of 32 percent chitosan and 68 percent finely milled shell substrate. The shell substrate had an average grain diameter of less than 0.1mm and had a size distribution that was identical to sample nine in the Mastersizer analysis. This batch of beads were treated with a cross-linking reaction similar to sample 2, table 3.5.1. This gave the beads a ratio of cross-linking expected to be below fifty percent, most likely somewhere between thirty and fifty percent.

It is important to keep in mind that the shell substrate, which is an inorganic part, is expected to be the critical component for fast acting adsorption, which is why the focus was set on how calcium carbonate relate to the beads capacity in conditions with continuous flow.

How the bead material behave differently between conditions with still water and continuous flow can give useful indications regarding the mechanisms behind the adsorption of phosphate onto calcium carbonate.

Also a setup with continuous flow can to some degree demonstrate whether the bead material show potential for practical applications like industrial scale adsorption columns.

If chitosan as the organic part contribute with some adsorption capacity then the aspect of cross-linking ratio will lack accurate data, although general trends can still be visible. To measure cross-linking accurately will need more advanced equipment and procedures than this experiment, see [p. ?] for more on this subject.

The last step of preparation was to dry the beads at 50^{o}C before they were weighted, this weight was compared to the weight of the raw materials.

Simplifications

A number of simplifications was made in order to get an overview of how the process would turn out and which data to collect.

Cross-linking

One aspect of this cross-linking process is that it will affect the accuracy of the new dry weight if we consider that the rate of reaction is unrealistic to measure accurately in these given conditions. The amount of glutaraldehyde consumed was a crudely known quantity when preparing this batch of beads. The reason for this will be because of unknown competing reactions and to some limited extent the rate of glutaraldehyde evaporating from the solution when exposed to open air.

As an example of competing reactions we know that glutaraldehyde will most likely be able to react at a similar rate with conchiolin proteins present in the powdered shells, although these proteins make up an unknown but, most likely small portion of this material *(wikipedia, 2015)*.

Water content

The amount of water retained by chitosan after the production and drying of the bead material can be assumed to be reasonably close to the water ratio of the raw chitosan from the supplier.

Setup

Flow conditions

In this setup the water flow was driven by gravity alone since the column was supplied by a simple bucket and a tube with a fairly narrow diameter. With this setup, only the average fluid velocity was measured. From these data the adsorption is assumed to scale reasonably linear with the rate of fluid flowing past the beads, *figure 3.5.4*. The hydraulic diameter at the end of the column was constricted with a simple ball valve to keep a low rate of water flowing through.

Column dimensions

The column had a bed length of 425mm and an inner diameter of 21mm, this equal a functional volume of ~147,2ml.

The volume of swollen beads was found to be approximately 90ml, this gives a total void fraction of approximately 57,2ml which equal a packing porosity of 38,86 percent. Where porosity is the ratio of empty volume (void fraction) to total volume.

$$\varphi = \frac{V_{empty}}{V_{total}} \qquad \varphi = porosity$$

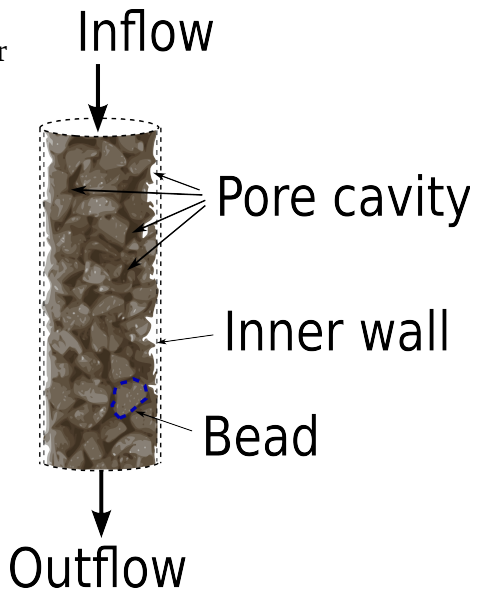

Figure 3.5.4

Bead material

This experiment was first conducted with 115g of swollen beads for two different rates of fluid flow, afterwards another three flow rates was used with a new set of swollen beads with a total

wet weight of 121,4g.

The dry weight of bead material for the first round was 69,66g, which gives a ratio of dry weight to wet weight of 60,6%. For the second round the dry weight was 73,54g with the same dry to wet weight ratio, table 3.5.5.

Table 3.5.5

Run	Start concentration	Substrate amount	Sample volume
1	0.25 mg/l	69.66g	540ml
2	0.28 mg/l	69.66g	952ml
3	0.28 mg/l	73,54g	2058ml
4	0.28 mg/l	73,54g	2000ml
5	0.30 mg/l	73,54g	2000ml

Methods of testing

Phosphate

The concentration of inorganic phosphate was measured with a *Spectroquant Nova 60* instrument from Merck. The difference in concentration of phosphate before and after exposure was compared to the rate of water flowing through the column and used as a basis for determining the beads adsorptive performance.

Flow

The amount of time for water to flow through was measured with a simple stopwatch and the total volume of water flowing through the system was collected in a bucket for measurement.

3.6 Test of durability, sample 1

Introduction

In this experiment the purpose was to carry out a simple stress test of the bead material to see if it would keep its structure after being subjected to mechanical stress for a extended period of time.

One key property of materials used in adsorption columns is whether they have a sufficiently rigid structure that make them practical to handle in larger volumes. There can be a significant amount of wear and tear as the beads grind against each other during both handling and column operation. If the beads break up into smaller units and finer particles there might be an increased risk of channel formation within the column.

Setup

50g of bead material was treated with a high amount of cross-linking similar to sample 1, table 3.5.1. The beads were submerged in 400ml of tap water in a 600ml flat bottom beaker and stirred by a large magnetic stirring rod for 72 hours.

4.0 Results

4.1 Analysis of particle size

The values for specific surface area (α), uniformity and obscuration for each sieve diameter is shown below in table 4.1.1. The raw shell substrate before milling is shown in figure 4.1.3, while the individual milled and sieved fractions of shell substrate is shown in figure 4.1.4.

Table 4.1.1

#	Sieve [mm]	α [m²/g]	Uniformity	Obscuration [%]
3	0,6	0.107	0,452	5.94
4	0,5	0.11	0,343	12.29
5	0,4	0.154	0,349	12.85
6	0,3	0.146	0,315	17.14
7	0,2	0.183	0,338	13.98
8	0,1	0.507	0,534	26.31
9	<0,1	0.785	0,769	17.93

Figure 4.1.3: Raw untreated shell substrate before milling.

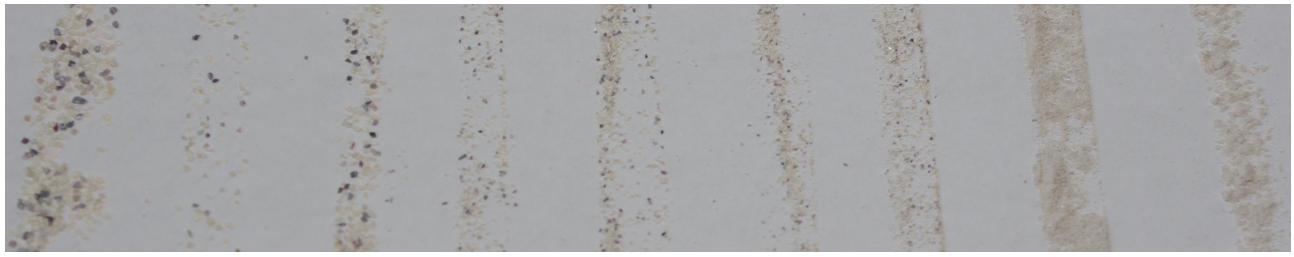

Figure 4.1.4: Fractions of sieved shell substrate, starting with sample 1 to the left and ending with sample 9 to right, table 4.1.1.

#3	Sieve: 0.7mm	

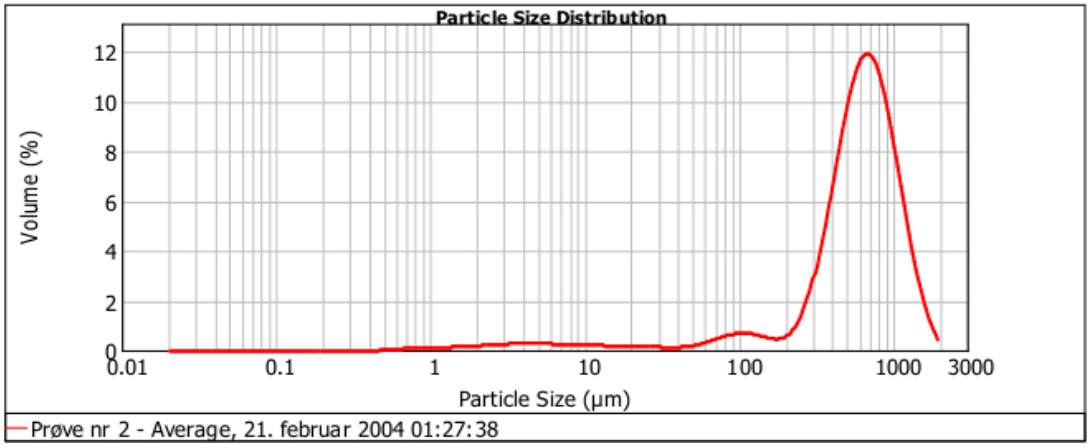

Figure 4.1.5: Distributions of particle size in terms of volume concentrations within sample 3.

#9	Sieve: 0.1mm	

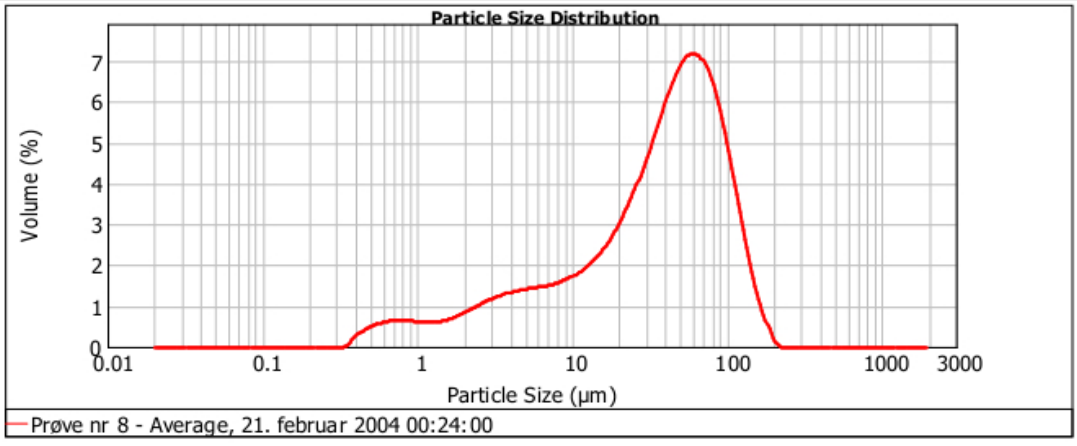

Figure 4.1.6: Distributions of particle size in terms of volume concentrations within sample 9.

Note: See table 4.1.1a and table 4.1.1b in attachment 1 for the whole set of data from the mastersizer analysis, as well as the complete set of graphs for sample 1 – 9 in table table 4.1.1c – table 4.1.1.e These data was not added in the result section due to limited their relevance.

4.1.1 Graphs of particle distributions, figure 4.1.5 – 4.1.6

A small portion of very small particles is visible for each fraction, this fraction is significantly higher in sample 3 *(figure 4.1.5, table 4.1.1)* compared to sample 9 *(figure 4.1.6, table 4.1.1)*. The increase in uniformity from sample 3 *(figure 4.1.5)* to sample 9 *(figure 4.1.6)* is visible on the graphs in the form of a larger portion of particles in the span from ~0.35µm to 40µm.

4.1.2 Uniformity, table 4.1.1, figure 4.1.7

The uniformity remains fairly similar for sample 3 to sample 7 *(figure 4.1.7)*, while it increases for sample 8 and 9 *(figure 4.1.7)*. Sample 8 has a 36% increase from sample 7, while sample 9 has a 56% increase from sample 9 has a 30% increase from sample 8, *table 4.1.1*.

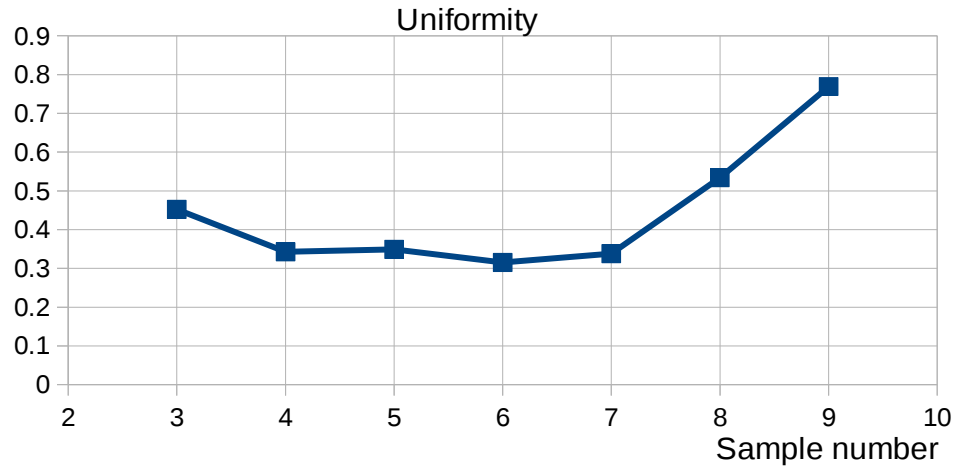

Figure 4.1.7

4.1.3 Obscuration, table 4.1.1, figure 4.1.8

Sample 6, 8 and 9 has the highest obscuration, where sample 6 has 17.14%, sample 8 has 26.31% and sample 9 has 17.93% while sample 3 has the lowest with 5.94%, *table 4.1.1*.

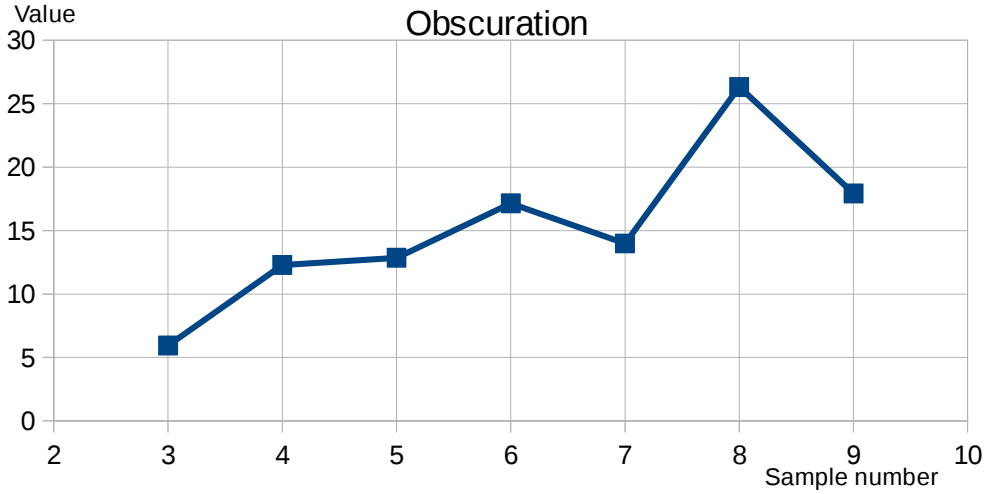

Figure 4.1.8

4.1.4 Diameter, volumetric weighted mean, table 4.1.1a, figure 4.1.9

The average particle diameter computed through *volumetric weighted mean*, decreases proportionally with the sieve diameter, *table 4.1.1a in attachment 1*.

The largest reduction in average diameter between samples occur between sample 4 and 5, as well as between sample 7 and 8, *figure 4.1.9*.

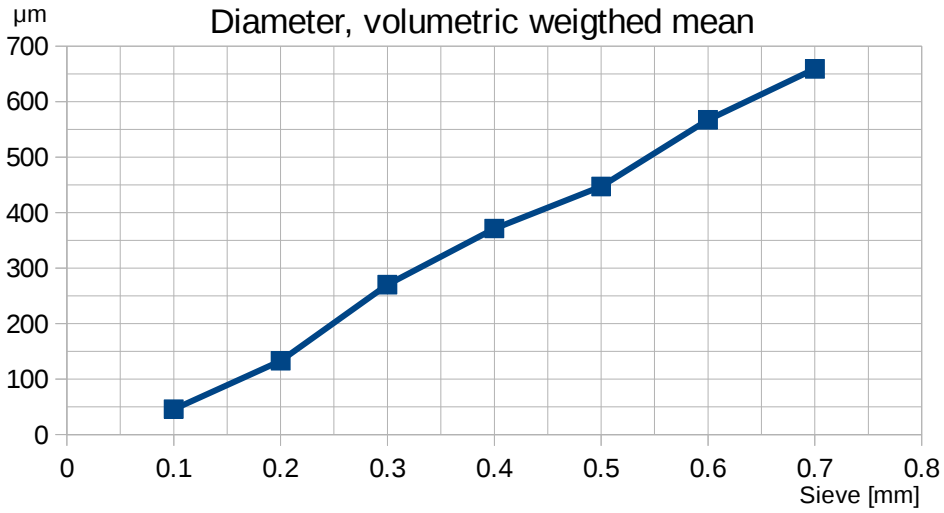

Figure 4.1.9

4.1.5 Specific surface area, table 4.1.1, figure 4.1.10

The largest increase happens between sample 7 to 8, where it increases from 0,183m²/g to 0,507m²/g, a difference of 324m²/g *(table 4.1.1)*. The second largest increase is between sample 8 and 9, where it increases from 0,534m²/g to 0,785m²/g, a difference of 0,251m²/g *(table 4.1.1).*

The lowest increase happens between sample 3 to 4 where it increase from 0,107m²/G to 0,11m²/g, a difference of 0,04m²/g, *figure 4.1.10.*

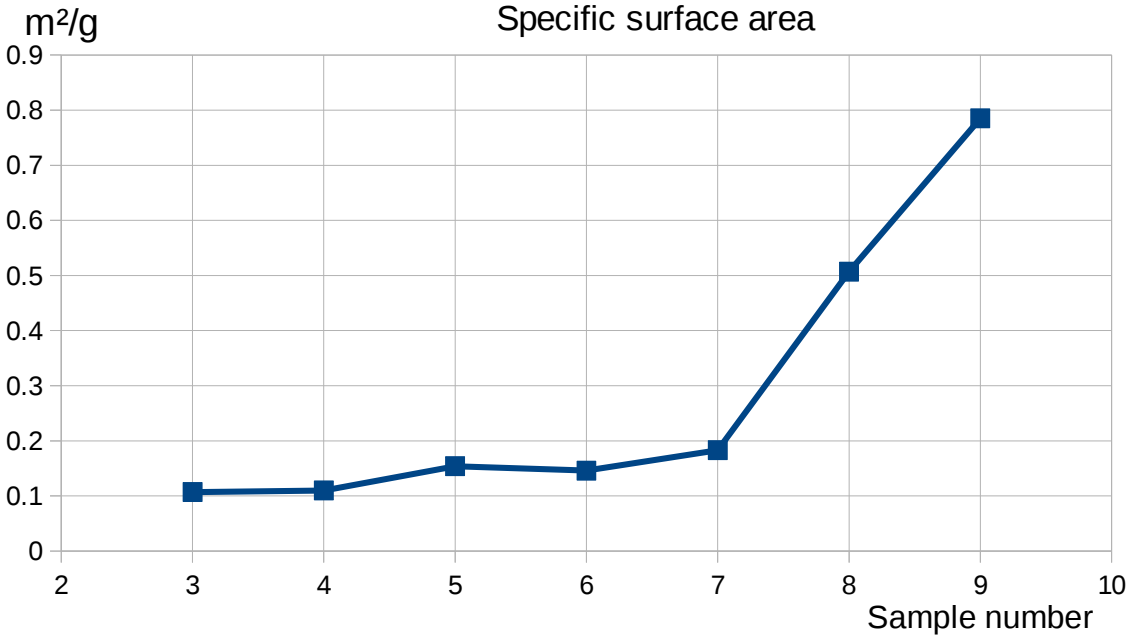

Figure 4.1.10

Note: See the attachments for the complete set of data from the particle analysis with mastersizer.

4.2 Adsorption – shell substrate

4.2.1 Series one, adsorption with effluent water, table 4.2.1

Table 4.2.1: This table list concentration after exposure and the equivalent ratio of adsorption per gram of sample $\frac{Phosphate\,[mg]}{Shell\ substrate\,[g]}$ *in*

	0	#1	#2	#3	#4	#5	#6
Phosphate [mg/l]	**0,18**	**0,13**	**0,115**	**0,095**	**0,085**	**0,065**	**0,05**
Difference [mg/l]	**0**	**0,05**	**0,065**	**0,085**	**0,095**	**0,115**	**0,13**
Phosphate adsorbed [mg/g]		**0,025**	**0,0325**	**0,0425**	**0,0475**	**0,0575**	**0,065**

The remaining phosphate after exposure decrease steadily from sample 1 – 6 where the last sample adsorbed a total of 0,065mg of phosphate per gram of milled shells, *figure 4.2.1 and figure 4.2.2.*

The highest increase in adsorption happens between sample 4 and sample 5 which increases from 0,0475 up to 0,0575 which equal a difference of 0.01mg/g.

Sample 6 is below the 0.05mg/l limit which put it at risk of being less accurate. At 0.05mg/l it fits well with the trend in the graph but, theris a chance it could be lower.

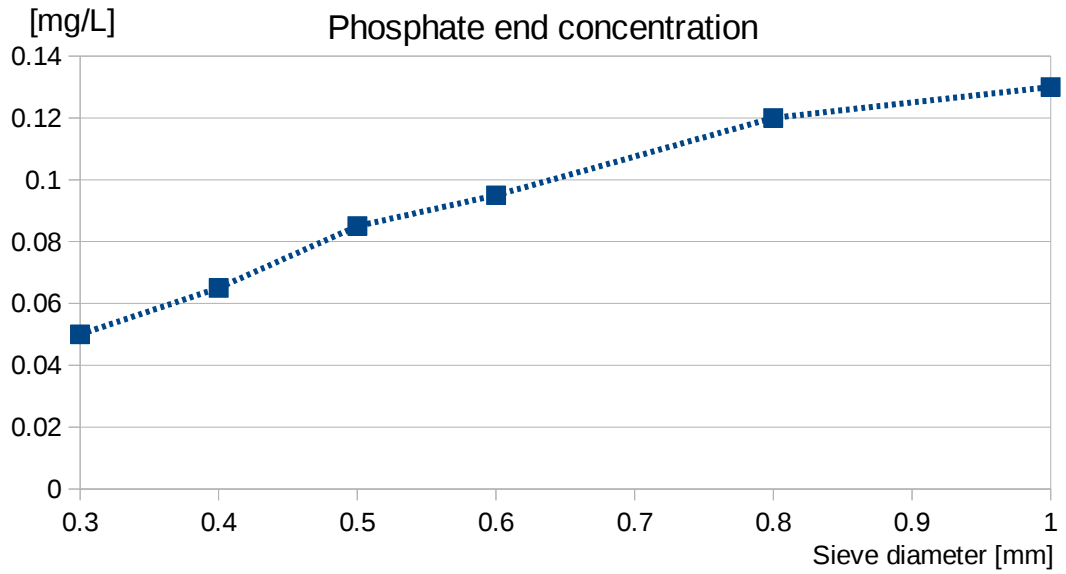

Figure 4.2.1: End concentration after shell substrate is added, start concentration was 0.18mg/l.

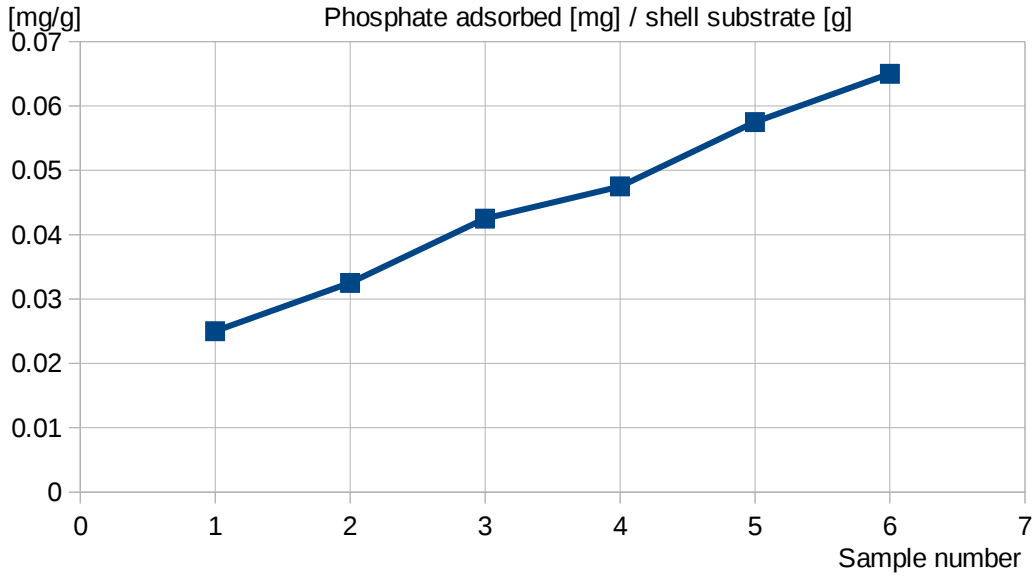

Figure 4.2.2: Adsorption in [mg phosphate/g substrate] for each sample

4.2.2 Series two, the influence of pH, sample 8 –9, table 4.2.2 – 4.2.3

Table 4.2.2: Sample 8 and 9 tested at different pH, results are shown as end concentration.

	Concentration [mg/l]		
pH	Start	End #7	End #8
6	0,15	0,12	0,11
7	0,15	0,12	0,11
8	0,15	0,11	0,1
9	0,15	0,12	0,11

Table 4.2.3: Results are shown as the amount of phosphate adsorbed per gram of shell substrate [mg Phosphate/ g shell Substrate].

	Adsorbed #8 [mg]		Adsorbed #9 [mg]	
pH	[mg]	[g/mg]	[mg]	[g/mg]
6	0,012	0,12	0,016	0,16
7	0,012	0,12	0,016	0,16
8	0,016	0,16	0,02	0,2
9	0,012	0,12	0,016	0,16

At normal pH conditions adsorption takes a leap and increases with 0,05mg/g between sample 8 to 9, figure 4.2.3.

There is a slight tendency for higher adsorption at pH 8. At pH 6 there is no measurable decrease in adsorption.

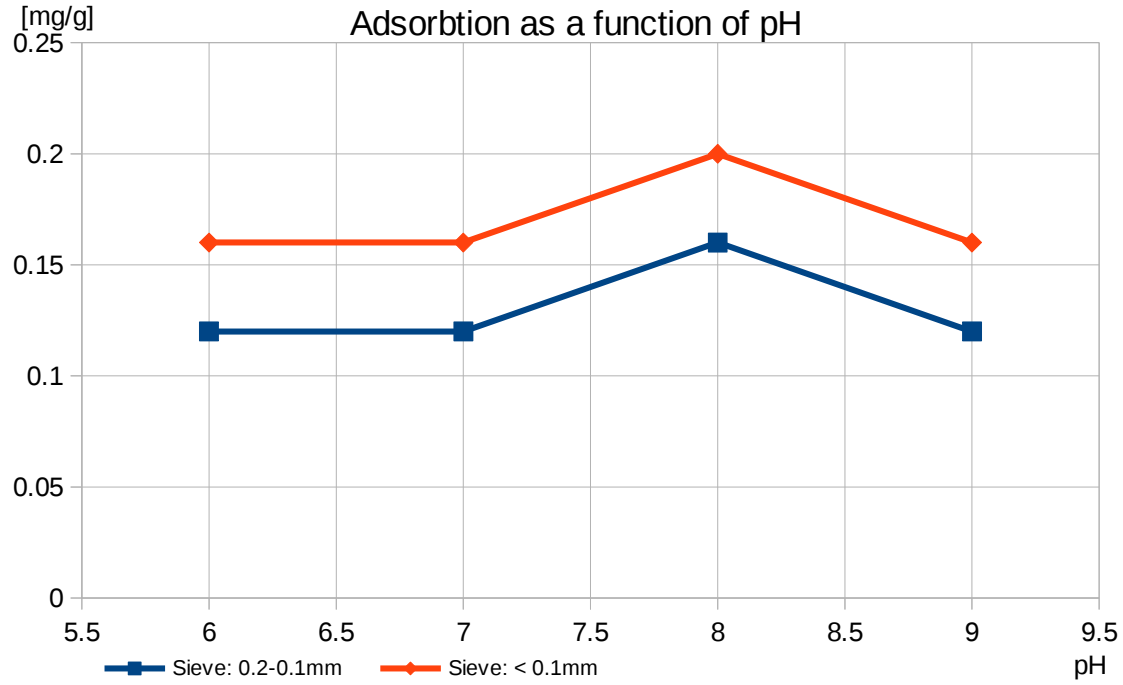

Figure 4.2.3: Similar to R.12, with [mg/g] for sample 8 and 9 at differnt pH.

If we take another look at the results from analysis of particle size, table 5.2.4, we see that the results for estimated specific surface [m^2/g] are in line with the results for adsorbed phosphate.

Figure 4.2.4 shows the values for specific surface area, table 4.1.1 are plotted against the values of adsorbed phosphate, table 4.2.1 and table 4.2.3.

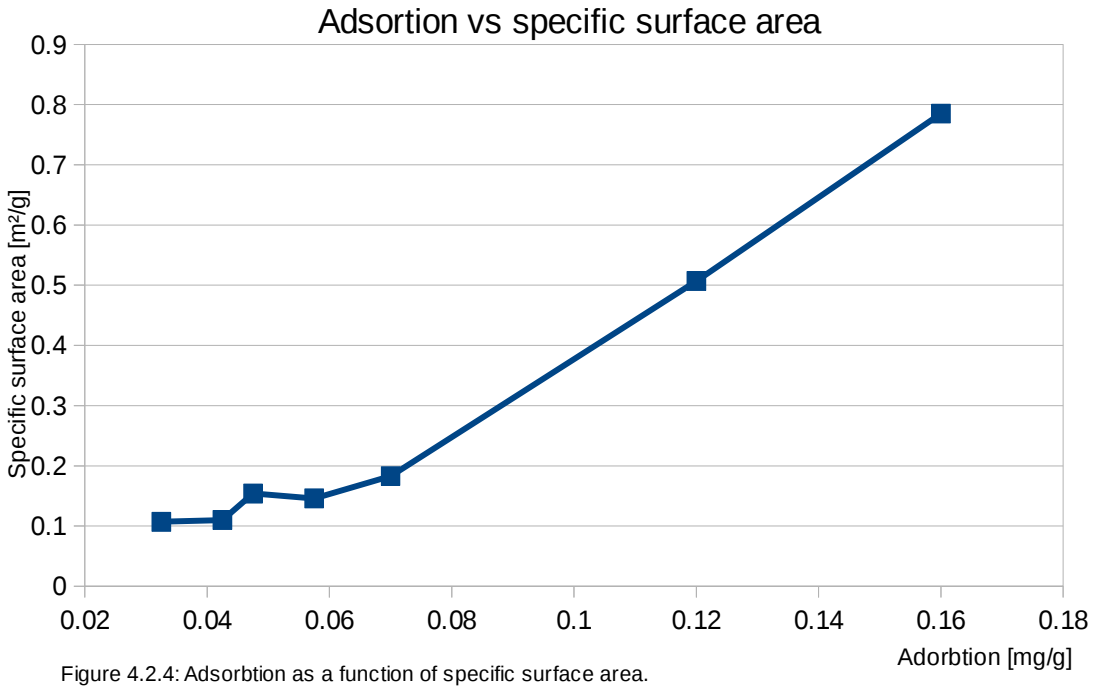

Figure 4.2.4: Adsorbtion as a function of specific surface area.

4.2.3 Series three, adsorption with diluted phosphoric acid

After exposure the phosphate concentration had changed from 3.44mg/l to 2.84mg/l, this equivalent an adsorption of 0.12mg in total.

In summary the adsorption per gram of substrate for diluted phosphoric acid was equivalent to 0.4 [mg Phosphate/g Shell substrate].

4.3 Adsorption – Bead material

4.3.1 Adsorption in batch

4.3.1.1 First batch, high cross-linking, Table 4.3.1

Table 4.3.1

Batch	Concentration		Difference
Water (200ml)	Start [mg/l]	Finish [mg/l]	Adsorbed [mg]
#1	0,28	0	0,0504
#2	0,31	0,11	0,036
#3	0,35	0,17	0,036
#4	0,35	0,34	0
Total			**0,1224**
Capacity [mg/g]			**0,0408**

From the first batch the process seemed to reach an equilibrium after the beads had adsorbed equivalent of 0,1224 mg of phosphate. This equals 0,0408 [mg phosphate/g bead material] and 0,06 [mg phosphate/g shell substrate]

4.3.1.2 Second batch, moderate cross-linking Table 4.3.2

Table 4..3.2

Batch	Concentration		Difference
Water (200ml)	Start [mg/l]	Finish [mg/l]	Adsorbed [mg]
#1	0,45	0,13	0,0602
#2	0,33	0,25	0,016
#3	0,25	0,17	0,016
#4	0,26	0,09	0,034
#5	0,23	0,07	0,032
Total			**0,1582**
Capacity [mg/g]			**0,0527**

After the first 72 hours the concentration had dropped from 0,45mg/l to 0,13mg/l,

With new water, after the next 48 hours we see a change from 0,33mg/l to 0,25mg/l, the water is replaced and the new start concentration is 0,25mg/l

After the second exchange of water the phosphate level drop from 0,25mg/l to 17mg/l.

The rate seem to increase after the third water exchange, with a change from 0,26mg/l to 0,09mg/l. This sample had one extra day of exposure, although equilibrium is reached before this. The increase in adsorption rate is approximately 50 percent, when comparing sample 3 and 4.

4.3.1.3 Third batch, low cross-linking, Table 4.3.3

Table 4.3.3

Batch	Concentration		Difference
Water (200ml)	**Start [mg/l]**	**Finish [mg/l]**	**Adsorbed [mg]**
#1	0,45	0,09	0,06945
#2	0,33	0,22	0,022
#3	0,25	0,12	0,02
#4	0,26	0,07	0,038
#5	0,23	0,05	0,036
Total			**0,18745**
Capacity [mg/g]			**0,0625**

After 72 hours the change was from 0,45mg/l to 0,09mg/l, this was equivalent to a difference of about 13.3 percent more compared to the beads with medium cross-linking.

This time with new water, after the next 48 hours we see a change from 0,33mg/l to 0,22mg/l, just like for the beads from sample 2.

After the second exchange of water the phosphate level drop from 0,25mg/l to 12mg/l, for the next water replacement the start concentration is 0,26mg/l for sample 3 beads.

Similar to the sample 2 beads, the third water replacement seem to have an equivalent increase in adsorption rate, where the changes was from 0,26mg/l to 0,07mg/l. The sample 3 beads continue to show better performance than sample 2 beads, with approximately 22 percent higher uptake.

Summary

The batch with full cross-linking was not carried out at the same timespan as the other two samples and so the data does not compare well for graphical illustrations. The second two samples on the other hand cam be used to illustrate the differences in adsorbed milligrams per round of fresh sample water.

If we look at the amount of phosphate adsorbed per gram of bead material we see that full cross-linking result in approximately $0{,}0408[\frac{mg\ phosphate}{g\ bead\ material}]$

When it comes to the batch with moderate amounts of cross-linking the adsorption performance increases to $0{,}0595[\frac{mg\ phosphate}{g\ bead\ material}]$ which is roughly 31 percent higher.

The bead batch with minor cross-linking showed even higher adsorption at approximately $0{,}0685[\frac{mg\ phosphate}{g\ bead\ material}]$ which is a difference of about 13 percent from the previous bead sample, *figure 4.3.1*.

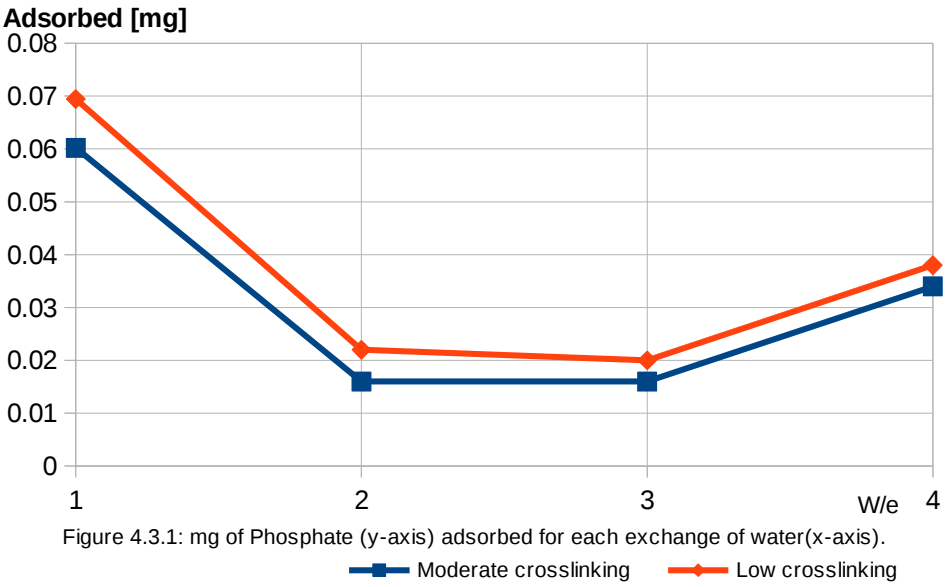

Figure 4.3.1: mg of Phosphate (y-axis) adsorbed for each exchange of water(x-axis).

4.3.2 Diluted phosphoric acid

After two days of exposure the phosphate concentration was measured to 2.77mg/L.

The total change in concentration was thus 0.74mg/L in other words to 0.296mg adsorbed from the 400ml of solution.

This gives an adsorption ratio of 0.296mg per gram of adsorbent material, the portion of shell material in this mixture was 68 percent which means the ratio of phosphate adsorbed per gram of shell material was equivalent to 0.4353 mg/g, this was slightly more than for the isolated shell substrate the value was 0.4 mg/g *(section 4.2.3)*.

4.3.3 Rate of adsorption in batch, table 4.3.5

Sample nr.	Time [min]	Concentration [mg/l]
1	0	0,25
2	2	0,25
3	4	0,23
4	6	0,23
5	8	0,23
6	10	0,23
7	12	0,22
8	14	0,22
9	56	0,18
10	69	0,17
11	89	0,17

Table 4.3.5 : Note the extended pause between sample eight to nine and between nine to ten.

There is an initial observable difference between sample two and three which occurs after four minutes, then there is no observable difference until twelve minutes has passed where the second drop in concentration occurs with another 0.01mg/l difference after fourteen minutes.

Between sample eight and nine there is another 0.04 mg/l difference although this happens after 56 minutes has passed since the start, the final drop happens after another 69 minutes with no observable difference for the next 20 minutes.

4.3.4 Adsorption in a column with continuous flow

4.3.4.1 First series, table 4.3.6.1, figure 4.3.6.1

Table 4.3.6.1

Flow			Phosphate			
Time [min:sec]	**Fluid volume [ml]**	**Flow [l/min]**	**In [mg/l]**	**Out [mg/l]**	**Diff [mg/l]**	**Adsorbed [mg]**
11:36	540ml	0,046552	0.25	0.15	0,10	0,054 mg
37:40	952ml	0,025274	0.28	0.16	0,12	0,11424 mg

The second test run had a flow rate was nearly half as large as the first run, with ~0,046 l/min for the first run and ~0,025 l/min for the second. This equal a difference at about 55 percent volume flow between the two.
This resulted in more than double adsorption for the lower of the two flow rates, with the first run only adsorbing 0,054mg and the second run 0,1142mg. This equal a difference of 47 percent between the two test runs.

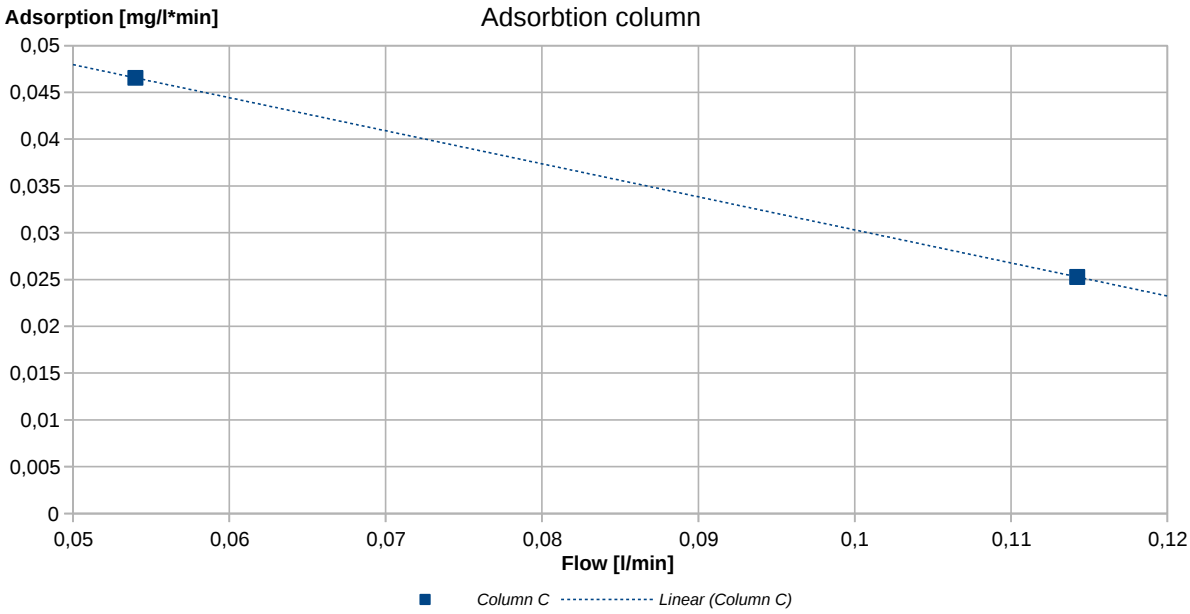

Figure 4.3.6.1

4.3.4.2 Second series, table 4.3.6.2, figure 4.3.6.2

Table 4.3.6.2

Flow		
Time [min:sec]	**Fluid volume [ml]**	**Flow [l/min]**
40:06	2058ml	0,0513217
52:45	2000ml	0,0379147
73:83	2000ml	0,027089259

Phosphate			
In [mg/l]	**Out [mg/l]**	**Diff [mg/l]**	**Adsorbed [mg]**
0.28	0.19	0,09	0,18522 mg
0.28	0.22	0,06	0,12 mg
0,3	0.22	0,08	0,16 mg

At the second test run there is a new batch of beads and we can observe an overall higher adsorption performance compared to the first test run, even though the flow rates are fairly close between the two series. The highest adsorption was at 0,185mg and the lowest at 0,12mg. The lowest adsorption in the second series was still more than twice as large as in the first series, even though the second series only had about five percent more beads. The highest adsorption in the second series also had the highest flow rate for both series.

The lowest adsorption happens at a flow rate of ~0,038 l/min which is close to the average value between the highest and lowest flow.

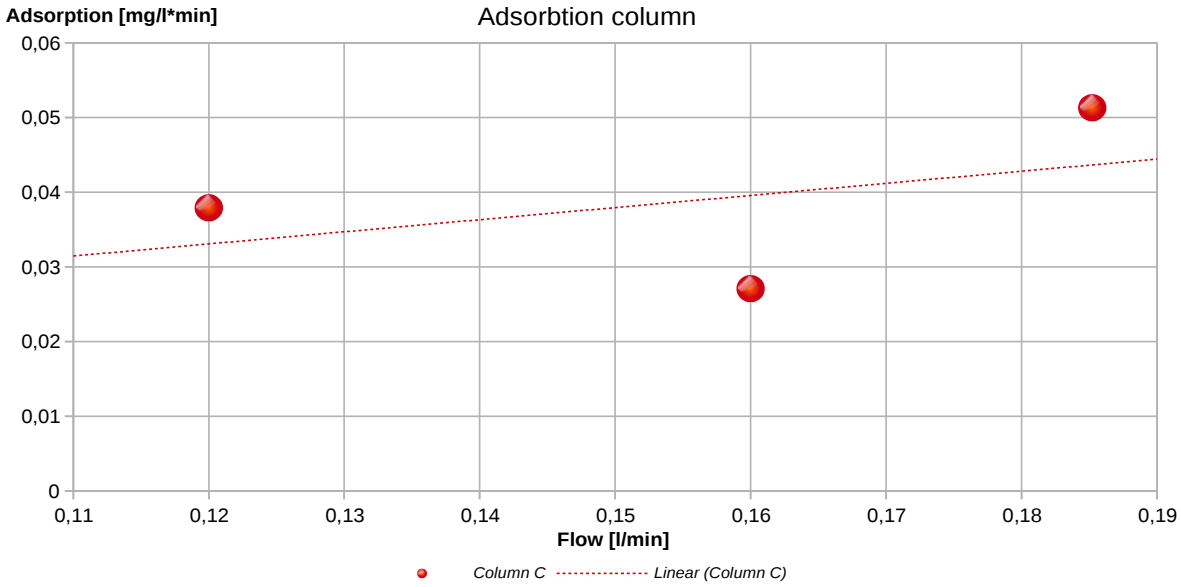

Figure *4.3.6.2*

4.4 Test of durability

After 72 hours with wear and tear from a magnetic stirrer the effects are visible in the form of rounded edges and smoother surface contours although the change in volume is minimal.

Figure 4..4.1

4.4.1 Swelling volume

Figure 4.4.2: Fresh beads without cross-linking in a dried state

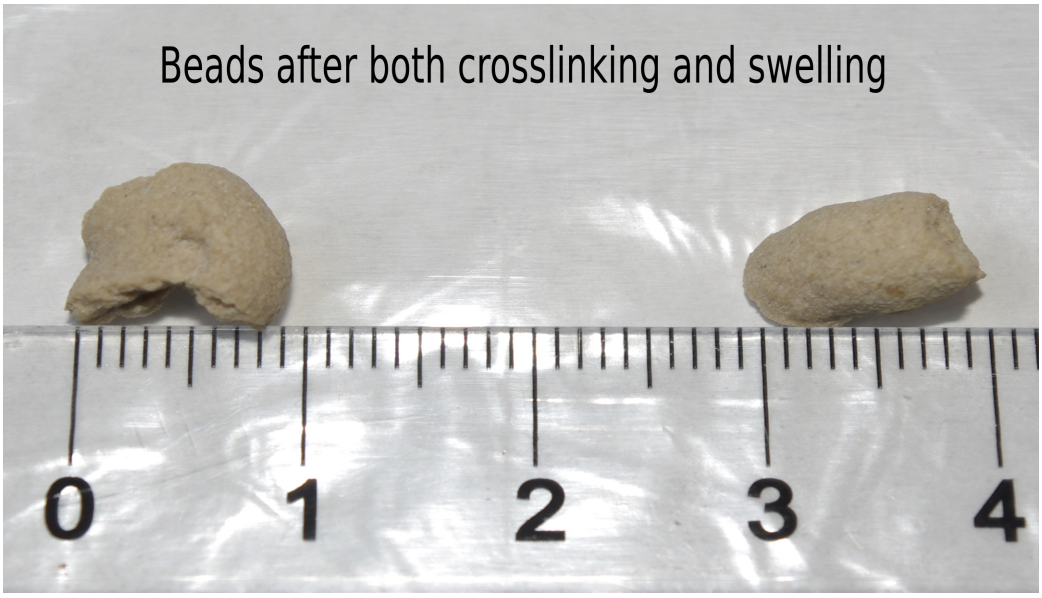

Figure 4.4.3: Fresh beads without cross-linking after being swelled in water.

Figure 4.4.4: Beads with a high amount of cross-linking after swelling, the cross-linking was similar to sample 1, table 3.5.1.

5.0 Discussion

5.1 Adsorption – shell substrate

When look at the finest sample with an estimated specific surface of 0.785m^2/g *(sample 9, table 4.1.1)*, we see that there is a considerable difference between adsorption in effluent water and the prepared solution containing phosphoric acid *(table 4.2.2 – 4.2.3, section 4.2.3)*.

The sample containing effluent water yielded a total adsorption of 0.2 [mg PO_4/g substrate] *(table 4.2.3)*, while sample containing the prepared solution yielded 0.4 [mg PO_4/g substrate] *(section 4.2.3)*.

The first and most likely influence for this difference is that the measurements carried out with effluent water had fairly low concentrations that were close to the minimum value for the instrument which has a measurement span of 0.05mg/l – 5mg/l. Like mention earlier, the samples can be expected to most accurate for values in the middle of this concentration span.

The samples with effluent water had both fairly low differences in concentration as well as fairly low start concentrations at 15mg/l and 18mg/l. This makes the accuracy more vulnerable to the effect of contaminants like dust particles, which increases the light adsorption registered by the optic instrument.

As an example, if dust particles in the sample increase the measured concentration value by 0.03mg/l, this would be equivalent for up to a 100 percent offset for sample where the actual change is from 0.15mg/l – 0.09mg/l but, where the measured difference is from 0.15mg/l – 0.12mg/l. For a sample with an actual change from 3.50mg/l – 2.80mg/l, a measured difference of 3.50mg/l – 2.83mg/l would only be equivalent to an offset of about one percent.

It is important to keep in mind that the sample with the highest estimated value for specific surface area was 0.785m^2/g. This can be compared to oyster shells, another natural resource from the mollusk family. In a study on oyster shells milled with a rotary knife cutter, (Tsai, 2013), the resulting product was found to have a specific surface area of up to 4.05 m^2/g while after further treatment with a planetary ball mill the specific surface area was further increased to 10.64 m^2/g. [19]

If the shell substrate used in the present study had gotten a similar treatment and archived a specific surface area of 10.64 m^2/g then the equivalent increase in adsorption capacity could be as high as 5.42mg phosphate adsorbed for every gram of milled shell substrate.

Considering that the start concentrations in the effluent water were fairly low, we can assume that the measurements performed with the prepared phosphoric acid solution give a more realistic picture of the substrates actual capacity.

5.2. Adsorption – Bead material

5.2.1 Adsorption in batch

Effect of cross-linking on diffusion

When comparing different degrees of cross-linking we can see fairly good indications that the degree of cross-linking seem to have an effect on the rate of diffusion. From table 4.4.2 it appears that the bead material with moderate cross-linking, had about 13 percent lower adsorption after 72 hours, compared to the substrate with least amount of cross-linking.

Unfortunately the bead material with full cross-linking, (sample 1, table 3.5.1) had no further change after the fourth liquid exchange, unlike the other two samples which had no observable difference after five water exchanges. This is not unlikely to be a result of microbial growth, considering how long time the bead material had been exposed in total, as well as the fact that any growth on the surface of the beads would be carried over with each water exchange.

However, if we compare bead material from sample 2 to sample 3, table 3.5.1, then there is a visible difference in phosphate levels after 72 hours, this gives us an indication that the pores in the polymer structure have shrunk and ions need more time to find their way through the polymer matrix.

This reduction in pore volume, will in turn increase the time it will take to fill up the last remaining portion as the material approach saturation. However this effect should largely depend on the ratio of outer surface area to volume, the internal diffusive resistance can be greatly reduced by molding the beads into a shape with low thickness *(section 2.7.5, Equation 2.7.5.6)*.

In *section 2.6.2* and *equation 2.7.5.6*, we could see that the effect of cross-linking could contribute to overall higher rate of diffusion for smaller sized beads. In the present study, figure 4.4.3 shows that the difference in in volume between bead material with no cross-linking and high cross-linking (sample 1, table 3.5.1) does not appear to be dramatic. The difference in volume between the samples of bead material with different amounts of cross-linking will be even less. This could indicate that there is macro pores within the bead substrate that are not as easily affected by the swelling ratio of the polymer. Taking this into consideration we can not conclude that the cross-linking is the deciding factor between the measured differences in adsorbed phosphate between
sample 1 – 3 (table 4.3.1 – 4.3.3).

Ion exchange mechanism or multistage adsorption?

Before the water is replaced the rate of adsorption is fairly low, when two measurements are performed 24 hours apart the phosphate concentration barely has any detectable differences. At this point it seem as if the system is close to having reached a state of equilibrium.

Then after the water is replaced, the adsorption rate increase considerably before seemingly reaching a new state of equilibrium.

This could suggests that the material behave as having a mechanism that involve the exchange of ionic species. For each time the water is replaced a balance appears to have been interrupted since the rate of adsorption increases, the most apparent explanation is that a significant amount

of counter ions has been removed from the system and resulting change in chemical potential drives more counter ions out of the bead material.

Another explanation is that the phosphate adsorption on calcium carbonate minerals is another type of multi- step process. Where the first stage is fast followed by a slower process which can last over a week. This has previously appeared to be the case for aragonite *(Millero, Huang, Zhu, Liu and Zhang, 2000).*

Microbial growth

Caution needs to be taken before drawing conclusions regarding the total adsorption capacity because growth of microbes could have an influence on the concentration of phosphate. The water was exposed to the bead material for several days in still water, microbes would have ample time to reproduce and consume some of the phosphate.

To compensate for this, a water sample of 1 liter was used for comparison to see if there would be any indications of loss while the bead samples were exposed. After four days the phosphate concentration decreases from 0.26mg/l to 0.23mg/l, even though there was no visible sign of algae growth.

When the water is exchanged every few days for the bead samples, there is a likely risk that the beads themselves might start to function as a growth medium, where a biofilm could form on the surface of the beads and drastically reduce any diffusion as well as the microbes starting to consume both phosphate and degrade the polymer.

This tiny experiment with stored effluent water give a significant indication that microbial growth had influenced the concentration of phosphate.

Capacity for phosphate adsorption

The beads with the least amount of cross-linking adsorbed significantly more than beads with a moderate amount of cross-linking. The reduction in cross-linking result in approximately 20 percent more adsorption after the third water replacement (*see table 4.4.2 and table 4.4.3).* However this difference could simply be a result of sample contamination considering that the effect of cross-linking does not seem sensible to be able to have such a large impact, especially since it would not be in proportion to the modest amount of chitosan present in the bead material, which was approximately 32 percent.

The apparent impact of cross-linking seen in this experiment will be inconclusive considering the visible signs of biofilm formation. If the substrate is coated with a bacterial film then this will most likely result in too much diffusive resistance for the active species, another factor is that microbes may also be able to consume free phosphate as nutrition.

Regarding maximum capacity

Unfortunately the maximum capacity was not reached when using effluent water for batch adsorption, there was indications of increasing microbial growth in the bottles used for the experiment which started to raise doubts as to whether continuing the experiment would yield accurate results.

When pure diluted phosphoric acid was used instead, the capacity was measured to be

approximately 0.435mg per gram of shell substrate in the beads, this is a moderate improvement from the pure shell material at 0.4 mg/g.

First of all, provided that the measurements are reasonably accurate, this may not guarantee that the capacity does not suffer from using chitosan as a binding material. This result does however give a strong indication that the capacity of the shell material remain close to intact and that the chitosan act as an active adsorbent that add some small amount of extra capacity as predicted.

In the experiments carried out here *(table 4.3.1, table 4.3.2, table 4.3.3 and section 4.3.4),* the shell based substrate should be able to gain much more specific surface area if the substrate was milled to finer degree with more specialized equipment. Considering this as well as the fact that the shell substrate is not made up entirely of calcite, there is much room for improvement when it comes to expanding the capacity of the bead material, (Tsai, 2013).

5.2.2 Adsorption in a column with continuous flow

Second series

The first test run had fresh unused beads, this is perhaps the most apparent reason for why this test run had both the highest rate of water flowing around the beads and the highest amount of phosphate adsorbed. Unused beads will have full capacity all the way from the surface to the center, which makes the adsorption happen very quickly for the outer layers, where the diffusion resistance is at its lowest.

In the third test run, the adsorption was higher than the previous run which indicates that the adsorbed phosphate diffuses between active sites and distribute itself evenly through the material until the concentration becomes homogeneous.

In simplified terms it can be seen as the energy of adsorption dissipating though the material, a bit like the way heat from a hot spot is spread in all directions until the material reach an equilibrium temperature with its surroundings.

Although the second series of test runs had overall higher adsorption, this could indicate that the average effective thickness of the beads was somewhat lower than the first round. The effective thickness is most likely to be the rate limiting factor or "*bottleneck*".

When comparing the results from the setup with an adsorption column to the setup run as a batch with time dependent testing of concentration, the most apparent difference is the rate of change.

The phosphate concentration drop significantly in a matter of minutes for a column with continuous water flow, this does not happen as fast when when the water is stationary like demonstrated in the previous experiments. When the water was stationary it could take up to an hour before there was any measurable difference in concentration.

This indicate that there might be a diffusion mechanism going both ways between the bead material the fluid, if there is an ionic species that needs to diffuse out of the bead before the phosphate can diffuse in, then the overall rate will likely be slower than if the process was only waiting for phosphate to find it's way in. Although these two process' are closely related, the profile for the chemical potential will still be different. If the fluid is stationary then the adsorption process will be limited by the passive diffusion of counter ions between the bead material and the bulk fluid. The reason for this is because the difference in concentration

between the fluid making up the surface film and the fluid in close proximity will be greater if there is a constant exchange of bulk fluid like there is in a adsorption column. If the bulk fluid is stationary then the concentration will decrease with the distance from the bead surface more slowly than if this fluid was being exchanged constantly.

6.0 Conclusion

In this project we have seen that milling of shell substrate will increase its capacity for adsorbing phosphate from water. This capacity will also increase as the shell substrate is milled into smaller and smaller particles.

The results in this project did not find any reduction in the shell substrates capacity for adsorbing phosphate when it was bound in chitosan, although this mixture did not perform as fast as the shell substrate alone.

When this mixture was molded into beads and used with continuous flow we could see that the adsorption process had potential for practical applications as the adsorption process turned out to be faster than expected under conditions with running water.

All in all the results have shown that a mixture of shell substrate and chitosan have the potential to be a viable option when it comes to applying the powdered shell substrate to effluent water, without having to use sedimentation tanks or centrifuges in order to separate the powder from the effluent water afterwards.

7.0 Further work

This project has only tried to map the basic properties of beads made of shell substrate and chitosan. There is much room for improvement on every aspect of this composite material, the first thing that comes to mind is how the beads are molded, the first priority should be to find an optimal ratio between the two base components as well as an optimal shape that maximizes the ratio of surface area to volume. This would most likely to wonders for the diffusive properties of the material.

The type of molding is inevitably linked to the amount of cross-linking is being used, smaller and thinner bead shapes might have to survive more wear and tear which is where cross-linking comes into the picture. More cross-linking makes the material more structurally rigid, but glutaraldehyde which was used in the present study might not be the best suited type of cross-linker. Fortunately there are several known alternatives like alginate, epichlorohydrin, citric acid among others, the type of cross-linker or a mixture of different cross-linkers can be studied to adjust the rate at which the end product will decompose naturally.

When it comes to producing beads themselves, there is no question that there should be more economic and efficient ways to produce beads than the way it was done in the present project. Using less hydrochloric acid, sodium hydroxide, water and drying should have a significant impact on the production costs.

In this project we saw that microbial growth could be a potential problem when it is being applied in larger scale, if this turn out to be a problem then different additives and cross-linking

will need to be explored further. The exact mechanism behind the adsorption should be investigated further, since a better understanding of the process is needed in order to determine whether the process is purely an adsorption phenomenon or if the process also involves exchange of ionic species between the bead material and the effluent water. There might also be other additives than can improve the adsorption mechanism between phosphate and calcium carbonate, as other studies has suggested (*see section 2.5.1*[11]). Chitosan is a very versatile material that opens up many opportunities to make different adsorbents that remove other compounds than phosphate. Cross-linked chitosan can hold a very wide range of both organic and inorganic materials, this project was after all inspired by another study to begin with.[1]

8.0 References

1. Auta M., Hameed B.H.(2013), Chitosan–clay composite as highly effective and low-cost adsorbent for batch and fixed-bed adsorption of methylene blue, *Chemical Engineering Journal*, Volume 237, Pages 352–361 [1. February 2014],

2. Malvern Instruments Ltd., *Mastersizer manual*, (1997), Ch 3. p.45.

3. Merc, S*pectroquant Nova 60 manual*, (2009), Merc, Ch. 1, p.2.

4. Merc, *phosphate cell test manual*, 1.00474.0001, (2011), p.1

5. Mollusk shell (21 October 2014), Wikipedia, <http://en.wikipedia.org/wiki/Mollusc_shell#Structure>, [03.05.2015] [5]

6. Chitosan (23 January, 2015), Wikipedia, <https://en.wikipedia.org/wiki/Chitosan>, [February 20, 2015]

7. Chitin (17 February 2015), Wikipedia, <https://en.wikipedia.org/wiki/Chitin>, [February 20, 2015]

8. Filipkowska U., Jóźwiak T., Szymczyk P. (2014), Application of cross-linked chitosan for phosphate removal from aqueous solutions, *Progress on Chemistry and Application of Chitin and Its Derivatives*, Volume XIX, 2014 DOI: 10.15259/PCACD.19.01

9. Kildeeva N.R., Perminov P. A., Vladimirov L., Nokikov V.V, Mikhailov S. N.(2008), About mechanism of chitosan cross-linking with glutaraldehyde, *Russian journal of bioorganic chemistry*, ISSN 1068-1620, 2009, vol. 35, No. 3, pp. 360-369, Pleiades Publishing.

10. Karageorgiou K., Paschalis M., Anastassakis G.N. (2006), Removal of phosphate species from solution by adsorption onto calcite used as natural adsorbent, *Journal of Hazardous Materials A139* (2007), 447–452, (2007)

11. Millero F., Huang F., Zhu X., Liu X. and Zhang J.Z., Adsorption and Desorption of Phosphate on Calcite and Aragonite in Seawater, *Aquatic Geochemistry 7: 33–56*, (2001).

12. Liu Y., Sheng X., Dong Y., Ma Y. (2011), Removal of high-concentration phosphate by calcite: Effect of sulfate and pH, *Desalination 289* p.66–71 (2012).

13. Nasef & Ujang (2012), Chapter. 1: Introduction to Ion Exchange Processes, *Ion Exchange Technology I: Theory and Materials*, DOI 10.1007/978-94-007-1700-8_1, Springer Science+Business Media B.V 2012, p.17.

14. Mersmann A.(2011), Chapter 9.5: Adsorbtion Kinetics, *Thermal Separation Technology: Prinsiples and methods*, Springer-Verlag Berlin Heidelberg 2011, p. 501.

15. Inglezakis & Zorpas (2012), chapter 4: Fundamentals of Ion Exchange Fixed-Bed Operations, *Ion Exchange Technology I: Theory and Materials*, DOI 10.1007/978-94-007-1700-8_1, Springer Science+Business Media B.V 2012, p.121.

16. Rohindra D.R., Nand A.V., Khurma J.R. (2004), Swelling properties of chitosan hydrogels, *The South Pacific Journal of Natural Science 22(1)*, p. 32 - 35. (2004)

17. Fick's laws of diffusion (8 March 2015), Wikipedia, <http://en.wikipedia.org/wiki/Fick's_laws_of_diffusion#Fick.227s_first_law>. [10 March 2015]

18. NIST/SEMATECH e-Handbook of Statistical Methods, (30/10/2013), "Screening designs", <http://www.itl.nist.gov/div898/handbook/>, NIST/SEMATECH, <http://www.itl.nist.gov/div898/handbook/pri/section3/pri3346.hhtm>, [20 February 2015]

19. Tsai W.-T. (2013), Microstructural Characterization of Calcite-Based Powder Materials Prepared by Planetary Ball Milling, *Materials (2013), 6*, 3361-3372; doi:10.3390/ma6083361, (2013)

9.0 Attachments

Analysis of particle size

#	Sieve [mm]	D,v	D,s	α [m²/g]	Uniformity	C [%Vol]	D,v diff
2	0,6	659,1	55,9	0.107	0,452	0.0490	
3	0,5	567,3	54,6	0.11	0,343	0.1018	91,8
4	0,4	447,0	39,0	0.154	0,349	0.0801	120,3
5	0,3	371,3	41,1	0.146	0,315	0.1142	75,7
6	0,2	270,2	32,7	0.183	0,338	0.0751	101,1
7	0,1	133,0	11,8	0.507	0,534	0.0595	137,2
8	<0,1	46,6	7,6	0.785	0,769	0.0247	86,4

Table 4.1.1a

#	D(0,1)[um]	D(0,5)[um]	D(0,9)[um]	Span	C [%Vol]	Obscuration [%]	W.r [%]
2	202,0	623,2	1140,1	1.505	0.0490	5.94	5.94
3	306,1	553,1	887,0	1.050	0.1018	12.29	3.146
4	234,7	442,0	700,3	1.053	0.0801	12.85	2.790
5	218,1	363,6	560,8	0.943	0.1142	17.14	2.235
6	151,0	262,7	419,9	1.024	0.0751	13.98	1.239
7	5,1	127,5	247,6	1.902	0.0595	26.31	0.773
8	3,3	39,6	100,3	2.452	0.0247	17.93	1.841

Table 4.1.1b

#2	Sieve: 0.7mm	

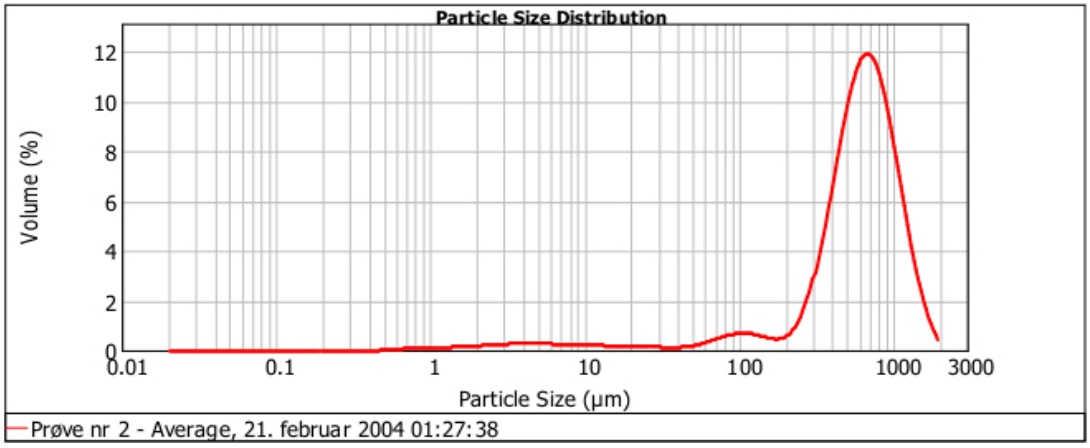

#3	Sieve: 0.6mm	

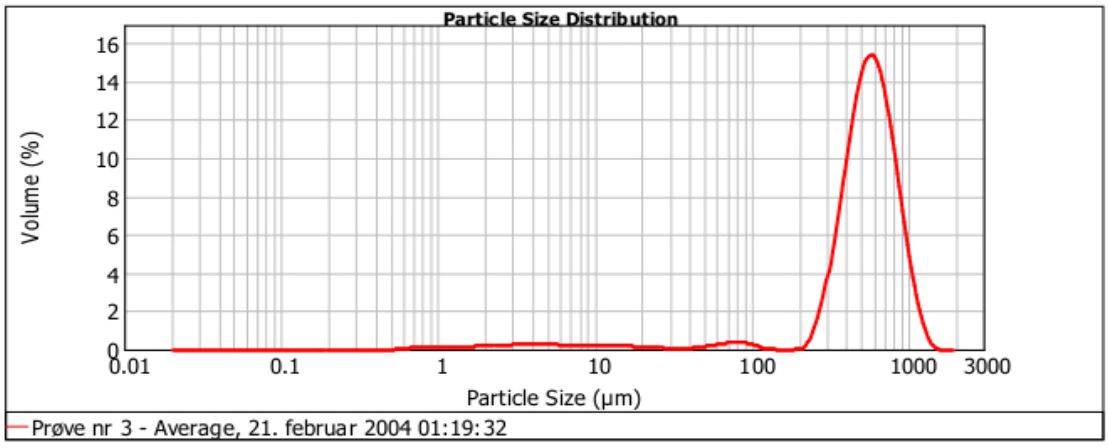

#4	Sieve: 0.5mm	

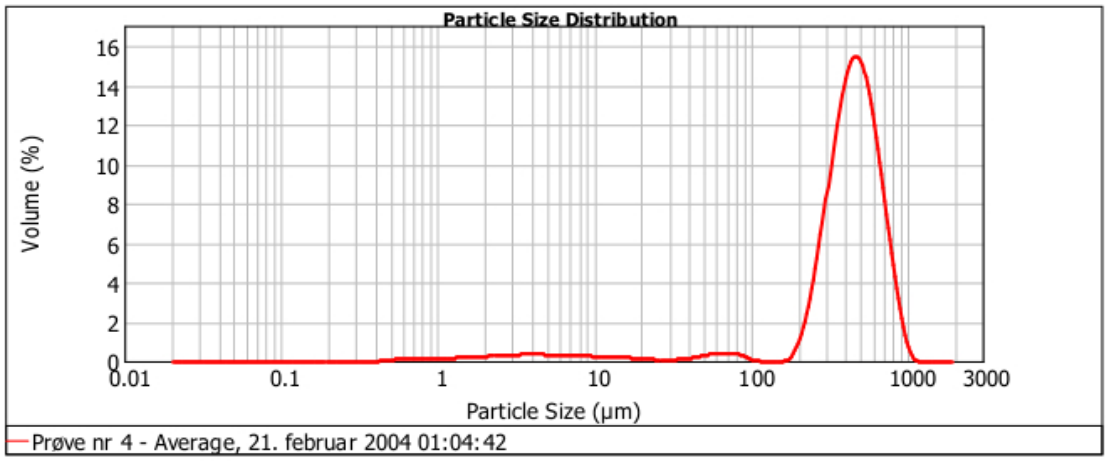

Table 4.1.1c

#5	Sieve: 0.4mm	

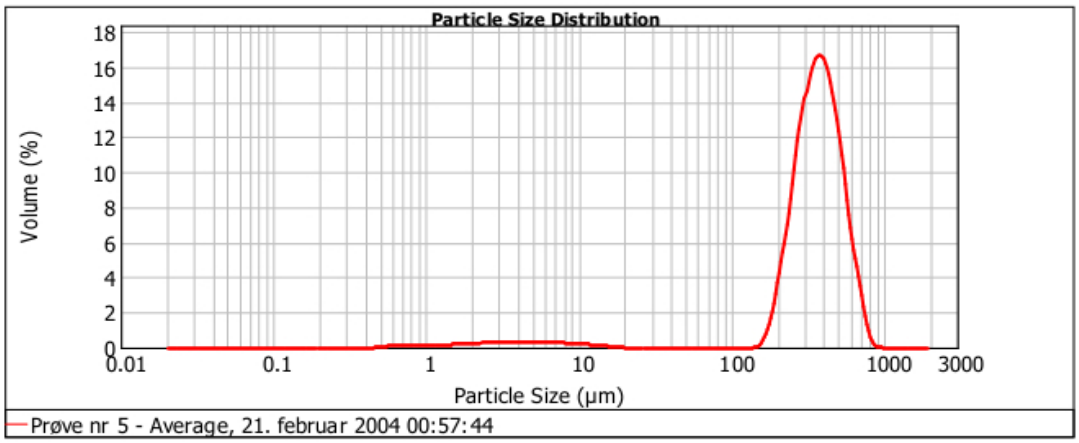

#6	Sieve: 0.3mm	

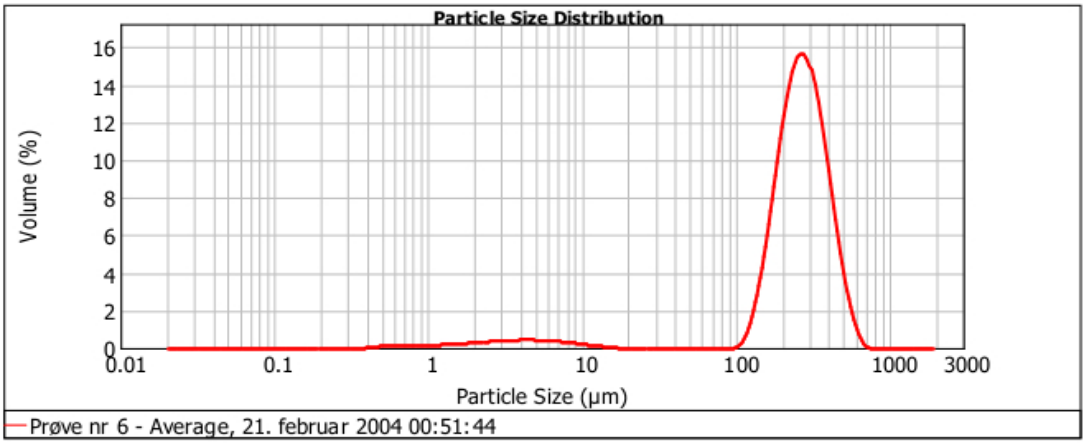

#7	Sieve: 0.2mm	

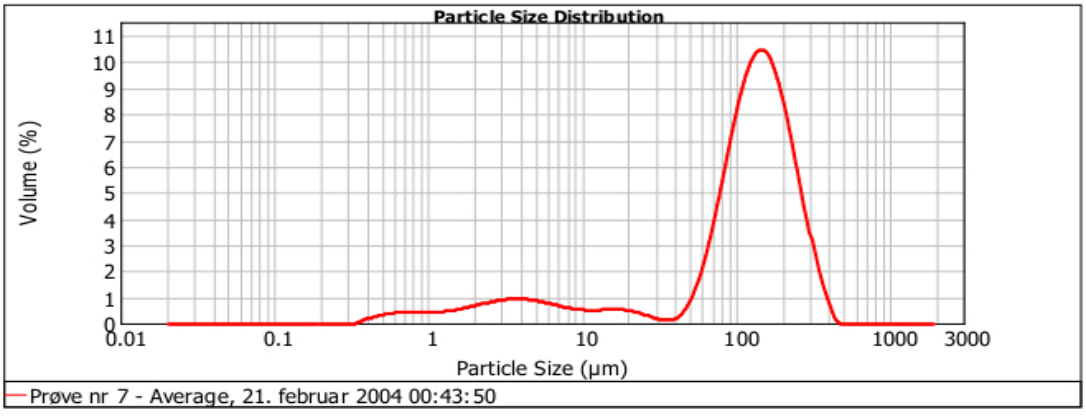

Table 4.1.1d

#8	Sieve: 0.1mm	

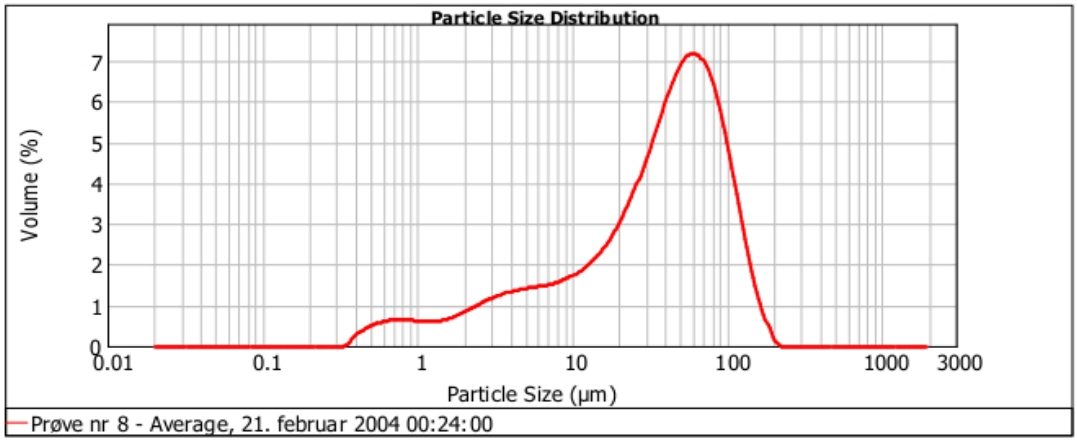

Table 4.1.1e

Norwegian University
of Life Sciences

Postboks 5003
NO-1432 Ås, Norway
+47 67 23 00 00
www.nmbu.no